



Prospects for improving the representation of coastal and shelf seas in global ocean models

Jason Holt¹, Pat Hyder², Mike Ashworth³, James Harle¹, Helene T. Hewitt², Hedong Liu¹, Adrian L. New⁴, Stephen Pickles³, Ekaterina Popova⁴, J. Icarus Allen⁵, John Siddorn², Richard Wood²

5 ¹National Oceanography Centre, 6 Brownlow Street, Liverpool, L3 5DA, UK

²Met Office Hadley Centre, FitzRoy Rd, Exeter, EX1 3PB, UK.

³STFC Daresbury Laboratory, Keckwick Lane, Daresbury, WA4 4AD

⁴National Oceanography Centre, European Way, Southampton, SO14 3ZH, UK

⁵Plymouth Marine Laboratory, Prospect Place, Plymouth, PL1 3DH, UK.

10 *Correspondence to:* Jason Holt (jholt@noc.ac.uk)

Abstract. Accurately representing coastal and shelf seas in global ocean models represents one of the grand challenges of Earth System science. They are regions of immense societal importance, through the goods and services they provide, hazards they pose and through their role in global scale processes and cycles, e.g. carbon fluxes and dense water formation. However, they are poorly represented in the current generation of global ocean models. In this contribution we aim to identify and quantify the important physical processes, and their scales, needed to address this issue in the context of the options available to resolve these scales globally and the evolving computational landscape.

We find barotropic and topographic scales are well resolved by the current state-of-the-art model resolutions (e.g. nominal $1/12^\circ$) and here the focus is on process representation. We identify tides, vertical coordinates, river inflows and mixing schemes as four areas where modelling approaches can readily be transferred from regional to global modelling with substantial benefit. We demonstrate this through basin scale northern North Atlantic simulations and analysis of global profile data, which particularly shows the need for increased vertical resolution in shallower water. In terms of finer scale processes, we find that a $1/12^\circ$ global model resolves the 1st baroclinic Rossby Radius for only ~20% of regions <500m deep, but this increases to ~90% for a $1/72^\circ$ model, so to resolve these scales globally requires substantially finer resolution than the current state-of-the-art.

We consider a simple scale analysis and conceptual grid refining approach to explore the balance between the size of a globally refined model and that of multiscale modelling options (e.g. finite element, finite volume or a 2-way nesting approach). We put this analysis in the context of evolving computer systems, using the UK's national research facility as an example. This doubles in peak performance every ~1.2 years. Using a simple cost-model compared to a reference configuration (taken to be a $1/4^\circ$ global model in 2011), we estimate an unstructured mesh multiscale approach resolving process scales down to 1.5km would use a comparable share of the computer resource by 2024, the 2-way nested multiscale approach by 2022, and a $1/72^\circ$ global model by 2026. However, we also note that a $1/12^\circ$ global model would not have a comparable computational cost to a 1° global model today until 2027. Hence, we conclude that for computationally expensive models (e.g. for oceanographic research or operational oceanography), resolving scales to ~1.5km would be routinely practical in about a decade given substantial effort on numerical and computational development. For complex Earth System Models this extends to about two decades, suggesting the focus here needs to be on improved process parameterisation to meet these challenges.

1. Introduction

Improving the representation of coastal and shelf seas in global models is one of the grand challenges in ocean modelling and Earth System science. Global ocean models often have poor representation of coastal and shelf seas (Renner et al.,



2009;Holt et al., 2010) due to both their coarse resolution and their lack of coastal-ocean process representation. In this paper we aim to identify the relevant physical processes that need to be better represented to improve this, quantify the horizontal scales needed to resolve these and explore the approaches that could be employed to achieve this. In particular we ask: at what point does a multiscale approach, which would allow increased resolution where required, become competitive
5 compared with a continued refinement of a global structured grid model? The multiscale approach could, for example, use unstructured meshes or multiple two-way nested grids. There have been other previous explorations of the scales important in shelf sea models (Greenberg et al., 2007;Legrand et al., 2007). These have tended to focus on specific numerical methods and approaches, largely around triangular unstructured meshes. Here we step back from a detailed analysis of the numerics and consider, in general terms, what is likely to be practical to achieve improved coastal and shelf sea modelling on a
10 global scale, on what time scales and what the ways forward may be.

The remainder of this section describes the background and motivation. Coastal-ocean processes and scales and their relation to global quasi-uniform model grids are described in section 2. Section 3 considers modelling approaches that might address coastal-ocean process representation and resolution. These are related to changing computer architectures and increases in performance in section 4 to estimate when they may be practical. The paper ends with conclusions in section 5.

15 1.1 Background and Motivation

Coastal and shelf seas represent a small fraction of the area of the global ocean (9.7% of the global ocean is <500m deep and 7.6% <200m), but have a disproportionately large impact on many aspects of the marine environment and human activities. While, our focus here is on modelling physical-ocean processes, this is often motivated by facets of marine biogeochemistry and ecosystems, as well as the climate system. These seas are the most highly productive regions of the world ocean,
20 providing a diverse range of goods (e.g. food, renewable energy, transport) and services (e.g. carbon and nutrient cycling and biodiversity), and also expose human activity to hazards such as flooding and coastal erosion.

The geography of these seas is very varied including semi-enclosed seas, broad open shelves, narrow shelves exposed to the open ocean, and coastal seas behind barrier islands. Rather than adopt a typological approach (e.g. Liu et al., 2010) we focus on generic physical processes described by some straightforward spatially-varying properties, as appropriate for the global
25 case; regional model studies would go beyond this to consider the detailed conditions specific to the region and tailor the model accordingly. While many of the largest shelf seas are in polar regions, we limit our investigation here to liquid water modelling and leave considerations of sea-ice modelling in this context to further work.

The study of coastal and shelf seas in a global context involves both upscaling (small scales influencing large) and downscaling (large scales influencing small) considerations, alongside the internal dynamics. The motivation for these is
30 now considered.

1.2 Upscaling

There are three key motivations to studying the influence of coastal-ocean processes on the global scale: dynamics, biogeochemical cycles and anthropogenic impacts (i.e. the large scale impact of small scale human activity). Here we consider some examples, without attempting to be exhaustive.

35 A particularly important dynamical feature is the formation of dense water on Arctic and Antarctic shelves and its subsequent downslope transport and mixing to form deep water masses through the “cascading” process, thereby contributing to the global thermohaline circulation.

Two key water masses in the global ocean circulation are Antarctic Bottom Water (AABW) forming the densest water masses in all the major ocean basins, and North Atlantic Deep Water (NADW) found predominantly in the North Atlantic,
40 lying above the AABW. Both these water masses are key components of the climate system, e.g. the NADW forms the lower limb of the Atlantic Meridional Ocean Circulation, responsible for the northward transport of large quantities of heat.



The AABW typically forms on the Antarctic shelves (primarily in the Weddell and Ross Seas, Adelie Land and near Cape Darnley) and subsequently cascades downslope into the deeper Southern Ocean (Orsi, 2010; Orsi et al., 1999). The source waters for the deeper component of NADW are mainly located in the extensive shelf seas of the Arctic and Greenland-Norwegian Basins, e.g. Deep Barents Sea Water forms through winter buoyancy loss west of Novaya Zemlya and cascades
5 down through the St Anna Trough to reach depths of 1500-3000 m (Aksenov et al., 2011).

While these water masses are of key importance in the global ocean circulation, it is presently difficult for models to represent the formation and cascading processes adequately. It is well known, for instance, that geopotential (z-coordinate) models will tend to mix too strongly (and spuriously) dense water masses cascading down shelf slopes, and models using isopycnic coordinates typically do not mix enough, through uncertainty about the specification of the actual mixing
10 processes involved (Roberts et al., 1996; Willebrand et al., 2001). This issue is also apparent in an analysis of CMIP5 coupled ocean-atmosphere climate models by Heuzé et al. (2013). This work showed that those (few) models that correctly produced AABW on the shelves were unable to cascade this water down-slope to the deeper ocean. Wobus et al (2013), however, have shown some success with a mixed z-s coordinate model (see below) in which s- (terrain-following coordinates) are applied over the shelf slope and facilitate the cascading downslope near Svalbard.

15 In terms of dynamical interaction with the atmosphere, coastal-upwelling (discussed further below) is seen as an important control of air-sea heat flux with implications for regional climate (e.g. in the southeast Pacific; Lin, 2007). On a smaller scale, coastal sea surface temperatures are a key influence on local weather (e.g. coastal fog and sea breezes).

A key role of the coastal-ocean in global biogeochemical cycles is the drawdown of carbon in highly productive shelf seas through photosynthesis (the ‘soft tissue carbon pump’) and its transport either to on-shelf sediments or off-shelf to the deep
20 ocean, where it is isolated from atmospheric exchange (Bauer et al., 2013; Chen and Borges, 2009). Alongside this export, nutrient rich waters are transported on-shelf, carrying properties reflecting the greater depths and longer timescales of recycling experienced by this water. This occurs either by an upwelling circulation or a combination of deep winter mixing and a downwelling circulation (Holt et al., 2009b), and helps support the coastal-ocean production and carbon drawdown. In addition the fixation of carbon through biogenic calcification (the ‘hard tissue carbon pump’), while largely unquantified,
25 would be expected to be particularly active in the benthic ecosystems of the coastal-ocean. Shelf seas are also a source of potent greenhouse gases, such as nitrous oxide (Seitzinger and Kroeze, 1998) and methane release from hydrates (Shakhova et al., 2010).

Benthic processes and the resulting benthic-pelagic fluxes are highly significant in the shallower shelf seas water column. Many physical processes influence benthic-pelagic exchange, relating to both the seabed characteristics (e.g. bed material,
30 presence of ripples) and the wave and current dynamics of the bottom boundary layer. The extent to which these influence coastal-ocean nutrient and carbon budgets on a global scale is largely unknown, but estimates (Bauer et al., 2013) suggest coastal-ocean sediments are a substantial carbon sink.

The coastal-ocean is the first point of entry for all material of terrestrial origin entering the marine environment, for example freshwater from rivers and ice sheets/shelves, inorganic nutrients, organic material and anthropogenic pollutants. This
35 material can be substantially modified as it is transported across the coastal-ocean. These transformations (ranging from simple mixing to complex biogeochemical interactions) influence the material’s ultimate fate. For example, whether the carbon and nutrients entering the marine environment from rivers (Seitzinger et al., 2005) reach the open-ocean depends on both the biogeochemical cycling on-shelf and the dynamics of the transit (Barrón and Duarte, 2015).

Hence the coastal- and open-ocean biogeochemical cycles are intimately coupled. There is still substantial uncertainty in
40 their role and feedbacks with the wider climate system, and making progress on this is largely dependent on the accurate simulation of the physical environment in the coupled coastal-open-ocean system.



1.3 Downscaling

Investigating the large scale impacts on smaller scale processes in the coastal-ocean can often be successfully treated by nested regional studies, focusing on an area of interest ranging from local (e.g. Zhang et al., 2009) to regional (e.g. Wakelin et al., 2009) to basin (e.g. Holt et al., 2014; Curchitser et al., 2005) scales. There are, however, occasions where a global or quasi-global approach is appropriate. These relate to cases where it is important to consider impacts on human systems of global relevance. Examples include food security and the role of Living Marine Resources in ensuring this. Fish and fish meal production are both connected via the global economy (Merino et al., 2012), so considering how climate change might impact them and hence food security requires at least a quasi-global approach (e.g. Barange et al., 2014).

Moreover, cases where basin scale oceanic processes directly influence the coastal-ocean are best considered on a global scale (Popova et al., 2016), as regional simulations may be compromised by errors propagating from simplified boundary condition approaches (see below). Coastal upwelling is a notable example. This is one of the crucial processes influencing shelf ecosystems, acting as an important source of nutrients and also supplying low oxygen and low carbonate saturation state waters (with consequences for oxygen state and acidification). Coastal upwelling driven by local wind stress (e.g. in eastern boundary upwelling zones) is amenable to regional modelling, accepting the need for accurate boundary conditions of larger scale nutrient distributions (Rykaczewski and Dunne, 2010). However coastal upwelling that occurs in response to the variations in strength of the boundary currents lying outside of the shelf areas requires a basin scale or global modelling approach. Western boundary currents are shifting polewards and intensifying, and their waters are warming two to three times faster than the global mean (Wu et al., 2012). A reorganisation of the coastal upwelling regimes is expected in these areas leading to the modification of the large-scale surface distribution of inorganic carbon and with significant consequences for living marine resources (Popova et al., 2016; Hobday and Pecl, 2014).

Another area that would benefit from a well resolved global approach is assessing the impacts of coastal-ocean sea level rise on a global scale; previous studies that have attempted to quantify the global cost of and vulnerability of coastal regions to sea level rise (e.g. Nicholls, 2004) have used coarse resolution global models and are limited in their ability to account for the regional variations in sea level rise that will strongly modulate its impact. Moreover, a global model with improved representation of the coastal-ocean opens up the opportunity to provide rapid assessments of a particular region, without needing to configure a new domain. Specifically, users of model-based services (e.g. reanalysis and forecast information) would be expected to benefit. Presently global or basin scale models are typically used to provide boundary conditions for bespoke regional/shelf systems that provide these reanalyses and forecasts. This may remain the best way to provide these services, given that local tuning and high resolution meteorological forcing would be expected to give improvements to model skill. However, it may be the case that acceptable if not optimal information could be provided from one global modelling service and this might satisfy user requirements in many cases, without the additional overhead presently required to provide regionally specific information.

2. Coastal-Ocean processes and scales

The distinct physical characteristics of the coastal-ocean, in comparison to other oceanic regions, are largely determined by their shallow depth and proximity to land. This has several implications for the dynamics:

- The water depth is generally similar to or not much greater than the surface or seabed boundary layers, so turbulence and mixing is invariably important.
- Incident waves grow in amplitude in shoaling water to conserve energy flux, so, for example, these can be regions of large tides.
- The bathymetric variation is of similar order to the water depth, so extreme variations in topography are common.
- The inertia (thermal and mechanical) of shelf seas is small, so they are highly constrained by external forcing.



- The horizontal length scales that dominate physical processes decrease with increasing depth (see below) and so are generally much smaller than in the deep ocean.
 - Rivers provide a source of buoyant fresher water that forms coastal currents and impacts stratification and mixing near the coast.
- 5 • In Polar Regions, land provides both a point of attachment (land fast ice) and a source of divergence (polynias) for sea ice.

Alongside these internal dynamics, coastal-open-ocean coupling is of critical importance to the considerations here. At ocean margins currents tend to follow contours of the Coriolis parameter divided by water depth (f/h), and so coastal regions are largely isolated from the large scale geostrophic circulation. Physical processes at the shelf break mediate the transfer of material across this barrier (Huthnance, 1995), e.g. the Ekman drain within the bottom boundary layer, eddies and internal waves; these tend to be fine scale and high frequency.

While there are numerous physical processes at work in shelf and coastal seas the underlying principles and equations are the same as in the open ocean. Their relative importance and scale differ significantly in the two cases, and so does how they are treated in numerical models. The processes are reviewed by Robinson and Brink (1998), Huthnance (1995) and Holt et al (In Press), so we do not discuss the dynamics in any detail here; we are primarily concerned with their characteristic horizontal scales (Table 1).

Ocean tides are a ubiquitous feature in the coastal-ocean, making a substantial contribution to the mixing and transport here; it is difficult to see how much progress can be made in the improvement of the representation of these regions in global models without some treatment of tides. The barotropic tide propagates on-shelf as a coastal-trapped wave (CTW), amplifying, and transferring energy to higher harmonics as the water depth shoals. Horizontally the scale of the propagating CTW (L_{bt}) is characterised by either their wave length or Kelvin wave scale, and so is resolved by moderate to high resolution global ocean models (see below). In contrast, the scale of rectification of tidal currents around topography and the periodic mixing and stratification at fronts is set by the tidal excursion (L_e , e.g. Polton, 2014), which is substantially finer.

Since they are regions of strong bathymetric variation, topographic steering of currents is a characteristic feature of shelf seas and ocean margins (e.g. the Dooley Current in the North Sea). The barotropic scale for these is simply the water depth divided by the slope (L_T) (Greenberg et al., 2007). Other topographic scales, such as the size of individual topographic features, will be locally relevant, but for simplicity here we focus on L_T .

The annual stratification cycle is a key feature of many shelf seas that are shallower than the winter ambient open-ocean mixed-layer depth. These are well described by a balance between surface heating and mixing (Simpson and Hunter, 1974). Where surface buoyancy input overcomes wind and tidal mixing (generally in deeper shelf sea waters), the water column stratifies during summer (e.g. in April-October in temperate northern hemisphere seas), while shallower waters remain well mixed throughout the year, excepting episodic stratification due to strong heating events or lateral sheared transport of buoyant fresh water. The general spatial pattern is then set by the propagation of tides across the shelf (i.e. the barotropic scales; L_{bt} , L_T).

The mixed and seasonally stratified waters are bounded by sharp tidal mixing fronts. These provide effective barriers to lateral transport, and drive baroclinic frontal jets (Hill et al., 2008), at a scale characterised by the 1st baroclinic Rossby Radius (L_1 ; Table 1). While mesoscale eddies are present in shelf seas (e.g. Badin et al., 2009) their importance in dynamics and transport on-shelf is much less clear than in the open-ocean (Hecht and Smith, 2008) or for ocean-shelf transport (e.g. Zhang and Gawarkiewicz, 2015). Coastal upwelling, and consequent frontal jets and filaments (Peliz et al., 2002), is a coastal-ocean process of substantial global importance; it also scales with the Rossby Radius.

Tidal flow over topography in a density stratified ocean excites internal waves at tidal frequencies (Baines, 1982), and their role in mixing at the shelf break (Rippeth and Inall, 2002) and in the vicinity of banks (Palmer et al., 2013) is now well



established. However, their relation to the various vertical mixing models currently employed is less clear. Much of the energy resides (at least initially) in the 1st mode, so their scale (L_{iw} ; Table 1) is closely related to L_1 .

Riverine and glacial freshwater inputs form buoyant coastal currents that can form a substantial part of the coastal-ocean circulation and an important control mediating the transport of terrestrial material, notably by inhibiting its direct off-shore transport. Their scale is difficult to quantify in general terms on a theoretical basis. Yankovsky and Chapman (1997) estimate the scale of a cyclostrophic plume, but this is highly dependent on detailed conditions at the river mouth, specifically the in-flow velocity (rather than transport) and the depth at the river mouth. Moreover, the flow then evolves as a ‘bottom trapped’, or ‘surface advected’ plume depending on prevailing conditions; these are difficult to evaluate in a global context. So instead, to characterise how well riverine coastal currents are modelled, we consider the minimum of two scales (L_r): the horizontal scale characteristic of seabed frontal trapping, defined as the depth of trapping (Yankovsky and Chapman, 1997) divided by the local slope and the inflow Rossby Radius (Avicola and Huq, 2002) (Table 1).

2.1 Coastal-ocean process scales in a global context

To put the scales described above and listed in Table 1 into a global context we calculate values using the global ORCA12 NEMO (Nucleus for a European Model of the Ocean) model (set up by the DRAKKAR group e.g. Marzocchi et al., 2015; Duchez et al., 2014) as a reference grid and bathymetry. This is a tri-polar grid with a coarsest resolution of 9.3km, but decreasing to minimum values of 1.8km in the southern ocean and 1.3km in the Canadian archipelago. The median scale is 6.3km. The bathymetry is a combination of GEBCO and ETOPO2. The process scales are themselves very much dependent on the scale of the information used to calculate them (e.g. the level of detail in topographic roughness in calculating, L_T), so a high resolution model grid used in practice, that does not have a North Pole singularity, is a good starting point. Figure 1 shows values of the barotropic (L_{bt}) and 1st baroclinic Rossby Radii (L_1), the topographic length scale (L_T) and the tidal excursion (L_e); see figure caption for further details of the calculation.

The barotropic Rossby radius is, as expected, large (>1000km) even at high latitudes, except in shelf seas and near the coast e.g. in 20m water depth at mid-latitudes, L_{bt} ~100km. For L_T , values <100km are widely distributed across the ocean, reflecting features such as ridges and sills. Values <10km are, however, restricted to the slopes at the ocean margins between the deep ocean and either the continents or the continental shelves. For the baroclinic Rossby radius (L_1) values <10km occur in high latitude oceans, whereas values <6km are limited to continental shelves. The tidal excursion (L_e) is much smaller, generally <10km. It shows an opposite pattern to the baroclinic Rossby radius, being largest at the coast. Where it is very small (e.g. in the open ocean) so is the tidal velocity and it is of minimal importance. Where it is large, however, it can make a significant contribution to local water column mixing/stability and fine scale residual transport.

To assess how model resolution compares with these scales we define a parameter:

$$e = L_x / (\max(\Delta x, \Delta y) \cdot E) \quad (1)$$

at each model grid cell of the ORCA12 mesh, i.e. the number of cells (size Δx , Δy) per length scale for process ‘ x ’. We multiply the size of each cell by a factor, E , to approximate other grid resolutions (without needing to generate the grids; e.g. $E=3$ for a nominal 1/4^o resolution). We focus on the barotropic and baroclinic Rossby radii and the topographic scale. We do not consider the tidal excursion further in this context, as resolving it is only beneficial in regions where the tide is large. Here we consider the nominal model resolutions listed in Table 2, along with example applications for the global and coastal-ocean cases. It is worth noting the current generation of forced, high resolution global models are of similar resolution to many historic and on-going shelf sea simulations (see references in Table 2). The cumulative distributions of e (Figure 2) then show the fraction of the model area at a particular resolution that resolves scale L with e or more grid cells. This figure also shows the distribution calculated just for water depth <500m i.e. the coastal-ocean. What constitutes adequate resolution then depends on the process in question. Hallberg et al (2013) suggest 2 grid cells per baroclinic Rossby radius gives a good representation of eddy fluxes, so we take $e > 2$ to be eddy resolving. If eddies have a characteristic size of



$\sim\pi L_l$ then we take $e < 2/\pi$ to be eddy excluding (i.e., a full parameterisation of eddy effects would need to be included in the model) and between these to be eddy permitting. For the barotropic Rossby radius (L_b) we take the limits on excluding and resolving to be $e < 2$ and $e > 10$, on the basis that this scale needs to be well resolved to capture many coastal-ocean processes (as discussed above). For the topographic scale we set the limits at 1 and 3 respectively, since at least three cells are required

5 to represent a topographically constrained jet.

We can therefore demonstrate that a $1/4^\circ$ global model is eddy resolving for 33% of the globe; this increases to 55% for $1/12^\circ$ and 80% for $1/36^\circ$. The fraction of the coastal-ocean that is eddy resolving is significantly less: $< 20\%$ at $1/12^\circ$; a $1/72^\circ$ resolution is needed to be eddy resolving over $\sim 90\%$ of the coastal-ocean. The topographic scale is much more promising. A $1/12^\circ$ model has $e > 3$ for $\sim 90\%$ of the global and $\sim 70\%$ coastal-ocean case. Resolving the barotropic Rossby radius is a

10 somewhat more stringent criterion than resolving the topographic scale in the coastal-ocean at $1/4^\circ$ or coarser resolution.

To explore the ability of models of different resolution to represent river plumes on a global scale, Figure 3 shows the cumulative distribution of the number of rivers (out of the 925 largest by volume flux; Dai et al., 2009) where the scale, L_r , is resolved to level e . This suggests modelling riverine coastal currents is an extreme challenge for structured grid global models. Using the same criteria limits as for L_r , at $1/12^\circ$ only 38 of the largest 925 rivers meet the ‘permitting’ criteria. This

15 implies that, while the fresh water balance is correct, its dispersion and transport properties will be limited. This number increases to 165 at $1/72^\circ$.

We see from this scale analysis that $1/72^\circ$ ($\sim 1.5\text{km}$) might be taken as a good target for resolving many small scale coastal-ocean processes such as eddies, upwelling and the largest river plumes. We would also expect it be adequate for resolving tidal excursions (where important) and internal tides. However, it is important to consider these results in the context of

20 coastal-ocean dynamics and previous modelling experience. Very few regional coastal-ocean modelling studies have been conducted at eddy permitting resolution, while still making significant progress in our understanding of the dynamics of these regions. Hence, while 1.5km might be seen as an aspiration, the practicalities of being eddy resolving on-shelf (when/how this can be reached are discussed below) should not be seen as a particular obstacle to making shorter term progress in modelling the coastal-ocean on a global scale. Some features with scales of the Rossby radius, such as coastal

25 upwelling, river plumes and frontal jets will still be present in models that do not resolve this scale, they will just not be particularly well represented. For example, continuity will lead to upwelling in a model of any resolution; its horizontal scale will be determined by the grid and numerics rather than the physics. Internal waves and eddies, in contrast, will simply be absent, and so need to be parameterised. The barotropic and topographic scales are vitally important for the accurate modelling of coastal-ocean dynamics, but can be reached at more modest global resolutions.

30 3. The Modelling Approaches

Here we consider, in general terms, how the processes considered above are *represented* by the model dynamical equations or specific parameterisations, and those that are *resolved* by the model grid.

3.1 Process representation

The representation of coastal processes in global ocean models is straightforward, at least in concept, for example the NEMO

35 model (Madec, 2008) has the capability of simulating both open ocean and shelf sea cases; this essentially allows these processes to be included by configuration selection as the global model resolution is refined. The open question is whether features pertinent to the coastal-ocean can be introduced into global models without degrading the solution in the open ocean or significantly increasing their computational cost. The model development process is largely focussed around reconciling the differences between coastal-ocean and global ocean approaches; a good guiding principle could well be to minimise the

40 changes needed in the global modelling approach, on the basis that these choices are well suited for the majority of open ocean processes.



The representation of tides in global models is the natural starting point. There are two approaches that can be considered: direct simulation and parameterisation. Along with tide generating forces, self-attraction, loading and solid earth tides need to be represented to achieve an accurate tidal simulation (e.g. Stepanov and Hughes, 2004). In addition the correct energy dissipation through bottom friction and internal tide generation is required. There have been several barotropic global tidal simulations, where dissipation is treated through parameterisations (see Stammer et al., 2014 and references therein). Beyond this, the issue for barotropic tidal modelling is largely one of resolution, which is readily achieved by many current configurations (Figure 2).

Baroclinic global tidal models with prognostic temperature and salinity (e.g. HYCOM; Arbic et al., 2012) can directly simulate the internal tide field. Around 60-90% of the energy (~1TW or 30% of the total barotropic tidal energy dissipation) transferred to baroclinic tides is in the form of low mode internal tides (Zhao et al., 2012). These can propagate large distances from their generation region, making their impact hard to adequately parameterise (Simmons et al., 2004). As energy is further transferred to higher modes and wave numbers, internal tides provide an important source of oceanic mixing (Munk and Wunsch, 1998). As identified above, global models at resolutions finer than $\sim 1/4^\circ$ permit low mode internal tides in the open ocean, but not higher modes or wave numbers or internal tides in the coastal-ocean. For example, Niwa and Hibiya (2011) find a strong resolution dependence of barotropic to baroclinic tidal energy conversion with no convergence even at $1/15^\circ$. Hence, some form of wave drag parameterisation may be required. Arbic et al (2012) found a carefully tuned wave drag parameterisation is necessary to accurately simulate tides in the isopycnal HYCOM model, whereas Muller et al (2010) found that a wave drag scheme was not required in the geopotential level MPI model. This contrast highlights a critical issue for the inclusion of tides in global models, namely spurious mixing, and the maintenance of deep water masses remains an issue in many ocean models (e.g. Ilicak et al., 2012). While physically realistic, the introduction of an energetic internal tide field may compound this numerical problem if not accompanied by efforts to reduce spurious mixing, for example through the use of advanced scalar advection schemes (e.g. Colella and Woodward, 1984; Prather, 1986) or adaptive vertical coordinates (Leclair and Madec, 2011; Gräwe et al., 2015).

If it turns out that addressing these issues is problematic or computationally prohibitive (e.g. for an Earth System Model), making direct tidal modelling undesirable, then the alternative is to use tidal mixing parameterisations, which can be straightforwardly adjusted not to overmix in the deep ocean. These make use of the increasingly fine resolution tidal information available from altimetry constrained models, e.g. TBX08 at $1/30^\circ$ (Egbert and Erofeeva, 2002). This is also required for global models that do not adequately resolve the barotropic length scales. The parameterisations should include benthic and under-ice mixing (Luneva et al., 2015), and mixing by baroclinic tides (St. Laurent et al., 2002). Allen et al (2010) explore using a 1D mixing model (GOTM) driven at each horizontal grid cell by imposed sea-surface slopes to estimate the vertical profiles of tidal shear. This has the advantage that it can accurately account for the interaction of tidal boundary layers and stratification, which is seen to be important, for example, in the Arctic (Luneva et al., 2015). Transport by tidal rectification is less easy to parameterise, but is expected to be secondary to the mixing effects on a global scale.

Vertical coordinates are a key consideration when modelling the coastal-ocean; the bathymetry necessarily varies substantially at the transition from open-ocean to shelf sea and from coastal seas to the land. Mixing processes (notably tides) require the accurate resolution of the benthic boundary layer, as do downslope flows such as cascades and Ekman drains. Moreover, bottom boundary mixing and freshwater input lead to exceptionally sharp pycnoclines. How vertical density structure changes on the transition from open- to coastal-ocean is clearly illustrated by two parameters: the pycnocline depth (Z_b) and thickness (Z_T). Here we use integral definitions:



$$\begin{aligned}
 Z_D &= \frac{1}{I} \int_{-H}^0 N^2 z dz \\
 Z_T &= \left[\frac{1}{I} \int_{-H}^0 N^2 (z - z_D)^2 dz \right]^{1/2} \\
 I &= \int_{-H}^0 N^2 dz \quad N^2 = \frac{g}{\rho} \frac{\partial \rho}{\partial z}
 \end{aligned} \tag{2}$$

where z is the positive upwards vertical coordinate, ρ the potential density, H the water depth and g the gravitational acceleration. These are readily calculated from observed profiles (here we use the EN4 data set; Good et al., 2013) and the global distribution of these parameters with water depth (Figure 4) shows a distinct pattern. The median pycnocline thickness increases steadily with water depth from ~2m (limited by resolution of the data) at 10m water depth to ~8m at ~300m, and plateaus at this value, only slowly increasing. The pycnocline depth shows similar behaviour, but does not plateau until ~500m. While EN4 is a very unevenly distributed data set, it clearly shows the influence of mixing from the bottom in sharpening and shoaling the pycnocline. To represent this in a model, it is highly desirable to increase the vertical resolution as the water depth decreases.

This need to increase resolution in shoaling water, alongside the need for smoothly represented across-isobath flows has led to a prevalence of terrain following (s -) coordinates in coastal-ocean models, accepting some exceptions (Maraldi et al., 2012; Daewel and Schrum, 2013) that have used geopotential (z -) coordinates. The large majority of global ocean models use geopotential or isopycnal coordinates. The reasons behind the lack of global s -coordinate models are the well documented issue of calculating horizontal pressure gradient and diffusion terms on sloping coordinate surfaces. Substantial progress has been made in addressing this (e.g. Shchepetkin and McWilliams, 2003), although bathymetric smoothing or hybrid coordinate approaches (e.g. Siddorn and Furner, 2013) are still needed to limit the coordinate slopes in many cases. Given the principle of minimising the changes to the model in the open-ocean, the natural choice (for a z -coordinate model) is to move to a hybrid system with z -coordinates in waters greater than a certain depth, transitioning to terrain-following coordinates in shallower water (Shapiro et al., 2013; Luneva et al., 2015). These can be formulated to match the original model's vertical coordinate system at the transition depth. Such an approach does require the use of a sophisticated horizontal pressure gradient calculation, but minimises the effect of any residual error from this term in the low dissipative open-ocean region where it is likely to be most harmful (e.g. in feeding spurious energy into the inverse energy cascade). Surface mixing processes of wind stress, convection and wave effects are common to open and coastal-oceans, and so the primary consideration for vertical mixing schemes in the coastal-ocean that differ from the open ocean is the need to accurately model mixing at the benthic boundary layer. Two equation turbulence models (e.g. k - ϵ) readily accommodate this and by using the Generic Length Scale approach (Umlauf and Burchard, 2003) these can be flexibly incorporated in a global model. While these approaches give good results in shelf seas (Holt and Umlauf, 2008), they differ substantially from schemes used in global models (e.g. the TKE scheme in NEMO and KPP scheme in MOM5). The implications for global ocean simulations, e.g. deep water mass preservation properties and maintenance of the meridional over turning circulation, have yet to be established, but could be readily tested in NEMO, since all three approaches are coded within it. Even with the highest resolution considered here parameterisation of riverine effects are still required for an accurate representation of their transport processes. This can be achieved by, for example box modelling approaches, as currently being tested in the Community Earth System Model (Bryan et al., 2015). To illustrate effects of introducing tides and hybrid vertical coordinate systems into a basin scale model (as an analogue of a global model) Figure 5 shows the summer potential energy anomaly (an integral measure of stratification; Simpson and Bowers, 1981) for three simulations with the Northern North Atlantic (NNA) NEMO (V3.5) configuration (Holt et al., 2014) compared with results from the global ORCA12 model. The simulations with tides and Z partial steps (ZPS), and with tides and hybrid Z - S (ZST) vertical coordinates both show the expected distribution of stratification and tidal mixing fronts (Holt



and Umlauf, 2008). The ZST has more vertical levels on shelf (e.g. 30 compared with 20 at 61m), and consequently higher stratification, notably in the central North and Celtic Seas. The extent of stratification is somewhat overestimated in the Irish Sea in ZST. In comparison, a parallel ZPS simulation without tides shows spurious stratification in regions that would be expected to be well mixed. The global model (also without tides) has well-mixed regions of more realistic extent, but still smaller than expected or seen in the models with tides. The discrepancy between the two models without tides can be accounted for by the global model using the TKE vertical mixing scheme. The TKE scheme is generally more diffusive than the GLS ($k-\epsilon$) scheme used in the NNA model, and so a deeper surface Ekman layer in the global model leads to an effect similar to tidal mixing in shallower water, but not as a product of the expected physical processes.

Quasi-horizontal mixing approaches suitable for both open and coastal-ocean require careful consideration. These schemes play two distinct roles: first to represent the effect of unresolved eddies in transport and second to complete the cascade of energy to unresolved scales. The former is particularly important in non-eddy open ocean models (Gent and McWilliams, 1990), but is not generally used in coastal-ocean models. The latter is common across both types of model, and is often treated as a stabilisation term without reference to specific physical principles. Both shelf and global ocean models tend to employ a combination of Laplacian and/or bi-Laplacian mixing for momentum and tracers. Mixing of temperature and salinity usually takes place along isoneutral, rather than geopotential, surfaces and this requires careful implementation in the case of sloping vertical coordinates and at fronts where isopycnals intersect the sea surface and bed.

As we see above global models span a wide range of dynamic scales and this is exacerbated when shelf seas are considered in detail; a quasi-uniform resolution model generally includes both eddying and non-eddying regions. Hence any model that aims to accurately cross these scales needs to account for the qualitatively and quantitatively changing nature of sub-grid-scale processes. This requires scale-selective approaches to determining sub-grid-scale diffusivities and viscosities (or other forms of closure). The simplest are just depth dependence (Wakelin et al., 2009) or based on horizontal shear (Smagorinsky, 1963). Combination of these with water column density structure (Hallberg, 2013) are likely to be most appropriate, but have not yet been tested in both the open and coastal-ocean contexts.

A final key feature of the coastal-ocean that needs to be considered is coastlines and related bathymetry (e.g. restricting exchange between regional basins). The treatment of the coastal topology is very much dependent on the horizontal gridding approach. Quadrilateral meshes approximate coastlines by imposing zero-normal flow condition on specific edges of the mesh and masking the landward solution. The resulting representation of the coast is highly resolution-dependent and leads to two specific issues. First the detailed representation of coastal features, e.g. at an inlet or a strait, is limited by this resolution; there is some limited scope to alleviate this through mesh distortion. Second, the staircase representation of a straight coastline impacts the fundamental numerical properties of the model, notably the propagation of Kelvin waves is retarded (Greenberg et al., 2007) and the accuracy of solution is reduced (e.g. from second to first order; Griffiths, 2013), even for coasts very closely aligned with the mesh, with only an occasional step. Available solutions to these issues for quadrilateral meshes are through shaved cell (Adcroft et al., 1997; Ingram et al., 2003) or immersed boundary (Tseng and Ferziger, 2003) approaches for high resolution models, or porous barriers (Adcroft, 2013) for coarser resolution models.

Triangular mesh models do not encounter these issues: they can fit the coastline with an arbitrary degree of accuracy limited by the minimum acceptable scale and accuracy of the geographic information. The representation of the details of the coastline is key advantage of triangular mesh models.

3.2 Resolving the pertinent scales

The most significant challenge in representing the coastal-ocean in global models relates to the small scales needed to represent the processes and geography (coastline, bathymetry, straits) of these seas. There are essentially two options for achieving a refined horizontal resolution: either increase the quasi-uniform resolution of the whole grid or introduce a



multiscale capability that allows refinement in specific locations. We consider briefly what these capabilities might be below, but first explore the balance between these two options if we desire to resolve a particular set of processes globally, refining the model locally to achieve this. We quantify this by building on the scale analysis above and define:

$$N_x = \sum (n/e)^2 = \sum (n \max(\Delta X, \Delta Y) \cdot E / L_x)^2 \quad (3)$$

5 to define the global sum of the number of cells needed in each global model grid cell to resolve a process, characterised by length scale L_x at a particular level (n). A constraint is imposed on this:

$$L_{\min} < L_x / n < \max(\Delta X, \Delta Y) \cdot E \quad (4)$$

10 The upper limit specifies a ‘base’ resolution, i.e. a multiple (E) of the global ORCA12 grid that is being refined. The lower limit, L_{\min} , acknowledges that there are limits to how fine a resolution is desirable, particularly in the case of scales that tend to zero with the water depth, and with respect to timestep constraints.

As an example, Figure 6 shows how a $1/12^\circ$ global grid might be refined to a minimum scale of 1.5km ($\sim 1/72^\circ$) as required by the above criterion, with L_x being the smaller of the baroclinic, barotropic, and topographic scales. Values at each cell range from $F^2 = (n/e)^2 = 1$ (no refinement) to $(\max(\Delta X, \Delta Y) \cdot E / L_{\min})^2 = 36$ in this case. Mid-latitude and arctic shelves require modest refinement ($\times 10$ -15 extra cells); the refined base mesh resolution of the tri-polar ORCA grid counters the reduced Rossby radius here. In some very shallow tropical regions the number is at or close to the maximum value, indicating that the desired level of process resolution is not always achieved. The accuracy of this estimate is limited by the underlying information (notably the bathymetry and the Rossby radius) and no consideration for refinement needed to resolve the coastline is made. Nonetheless this still provides a useful guide in terms of the relative cost of multiscale and globally-refined resolution approaches. Here we compare this calculation with the total number of grid cells in the globally-refined case (at L_{\min}). Because the minimum scale is the same for both no timescale factor is needed. This approach takes no account of the mesh structure needed. In particular there will be limits on how quickly scales can be allowed to vary on an unstructured mesh (see for example Figure 6 lower panels, show the change in resolution needed can be locally very abrupt) and so this puts a lower bound on the number of cells needed in the multiscale case.

25 We consider three values of L_{\min} : 9.3km ($\sim 1/12^\circ$), 3.5km ($\sim 1/36^\circ$) and 1.5km ($\sim 1/72^\circ$) (c.f. Table 2) in Figure 7. So for example, a $1/4^\circ$ global model refined where necessary to resolve the Baroclinic Rossby radius down to a minimum scale of 9.3 km has only ~ 5 times fewer cells than a global model at a nominal scale of ~ 9.3 km. This increases to ~ 16 and ~ 21 as the minimum scale is decreases to 3.5km and 1.5km respectively, and a $1/12^\circ$ model refined to minimum scale of 1.5km has 16 times fewer cells than a $1/72^\circ$ global model. The limiting behaviour evident from these plots arises because at coarse base resolution most of the grid is refined to meet the criteria (i.e. the base resolution becomes irrelevant), while at a fine base resolution this meets the criteria in many regions anyway and the refinement becomes less relevant.

A particular caveat of these results is that no account is made of the overhead in achieving this refinement (e.g. using a finite volume or finite element approach), which would be expected to be considerable and some estimate of this is made below. These results are considered in terms of what may be computationally practical in section 5.

3.3 Options for multiscale modelling

There is already a substantial literature on multiscale modelling and we do not attempt to review this here. We note that unstructured mesh approaches generally focus on triangular mesh models using a finite volume (e.g. FVCOM; Chen et al., 2003) or a finite element (e.g. FESOM; Timmermann et al., 2009) approach. MPAS (Ringler et al., 2013) is an important exception, being based on hexagonal meshes using a hybrid finite volume, finite difference approach. Danilov (2013) provides an account of the issues of unstructured mesh modelling, and what is clear from that review is that selecting an



solution approach or grid arrangement, for example, on the basis of lack of computational modes or formal accuracy is far from straightforward, and must be left to detailed investigations in idealised and realistic cases.

Quadrilaterals in contrast have good numerical properties (particularly for wave propagation), so a conceptually attractive option would be a mixed element grid, with quadrilaterals covering the majority of the ocean and triangles used to refine the grid where needed (Figure 9). The finite volume method is readily generalised to this approach, which would have the advantage of only requiring stabilisation of numerical modes in the triangular mesh region. However, the best choice of grid arrangement (Figure 9B shows some options) is uncertain. The C-grid type arrangement is the optimal choice for wave propagation in quadrilaterals, but has serious numerical issues for the triangular mesh. Hence, any choice will be a compromise and require careful evaluation. Currently Danilov and Androsov (2015) have investigated the B-grid and Holt et al (2013) the A1 grid cases. Alternative approaches for this are global triangular or hexagonal mesh models. The former have been available for many years, but have not yet reached a level of maturity where they form the ocean component of CMIP models, whereas the latter is an emerging capability (Ringler et al., 2013).

Structured grid models have scope for multiscale capability by distorting their horizontal coordinates and through nesting. Coordinate transforms generally limit the refinement to a single region of interest and requires considerable investment in model configurations (a new global model must be configured and tested); so this region must be likely to endure as a focus of interest. An example to facilitate regional impact studies is the use of a rotated polar grid (Gröger et al., 2012) to focus resolution on European seas. While this can address the downscaling issue for a single region, it does not help with the upscaling question, and may distort the global solution through its focus on one region.

Nesting is the most common approach to multiscale modelling. In its simplest form boundary conditions for a fine resolution regional model are taken from a previous run of a larger area ocean model. It has the significant advantage that the global model does not have to be rerun for each regional simulation. On this basis it remains an important approach for model development, and investigations of regional systems and their response. The general downside to nesting is the accuracy at which information can be exchanged between the two domains and the degradation of the solution at the boundary; it is usual to linearise the boundary conditions and to only exchange a limited subset of information at lower frequency than the model timestep. That said, there has been extensive work on regional model boundary conditions (e.g. Marsaleix et al., 2006; Mason et al., 2010) and by using a careful combination of active and passive approaches good solutions can be obtained. One-way nesting can be straightforwardly extended to a global scale using multiple regional nests (Holt et al., 2009a). The problem is simply one of standardising the configuration procedure and of managing workflow. However, one of the key advantages of regional models, that they can be tailored to specific conditions of a region, is generally lost in automatically configured domains. The underlying assumption to such one-way nesting is that feedbacks between the regional and global simulations are small, at least on the timescales of interest and again it only addresses the downscaling question.

A natural extension of the nesting approach, which allows for upscaling, is two-way global scale nesting. The AGRIF tool (Debreu et al., 2012) provides a capability to automatically generate nests, that has been utilised in both the ROMS and NEMO systems, generally with individual regions being refined with one or more nests. In theory this is extendable to the global scale, with multiple nests placed to locally resolve coastal-ocean processes. Several approaches exist to couple the two grids, reviewed by Debreu and Blayo (2008). Because this occurs ‘in memory’, these can be substantially more sophisticated than off-line nesting by file exchange, and essentially aim to link solution approaches in the two grids, coupling at the time steps of the respective grid. This means that as well as having two-way interaction, many of the issues associated with off-line boundary conditions noted above are alleviated, although noise and wave reflection are two issues that require particular attention. An issue with this approach in the global context is the restriction (for AGRIF) to rectangular domains (in model coordinate space; see below). This is somewhat inefficient and inflexible, and the coupling between neighbouring refined regions, with potentially different levels of refinement needs to be considered. Large irregularly shaped nests (e.g.



Holt et al., 2009a) would be good option, not over-refining in the open ocean and limiting the number of grids and connections between them. This would require substantial development to AGRIF or an alternative approach. An approach that has yet to be thoroughly explored is using model couplers (e.g. OASIS3-MCT) as a 2-way downscaling tool. This would allow complete flexibility between nests, e.g. a different executable can be run in each nest, but whether the coupling system is sufficiently efficient to permit coupling at the model time-steps is unclear.

To put global nesting in the same context as the above scale analysis, we consider a multi-block approach (accepting the limitation to rectangular domains for now), and consider the global grid ORCA12 grid divided into $\sim 15^\circ \times 15^\circ$ blocks. Each of these is then given a refinement level E^2 ranging from 1 to 36, as above. To provide a representative maximum value (but not set by a very few large grid point values), this is taken to be the 95th percentile of the grid cells in each block. To mimic the AGRIF refinement process each block takes an integer value: $(\text{int}(F))^2$. This example leads to 194 out of 344 cells requiring refinement (Figure 8). Such a setup would be a challenging computational engineering effort and certainly less elegant than an unstructured mesh approach, but is likely to be more efficient (quantified below) and is available as an evolution of well tried and tested global modelling approaches, rather than a completely new direction. Whether it is more or less accurate than a comparable finite volume or element approach must be left for future investigation.

4. Utilising the computational resources: potential future configurations

Ocean modelling has benefited from the general exponential growth in High Performance Computing (HPC) capability, with the largest machines approximately doubling in performance every 18 months since 1993 (TOP500¹ list). There are two technology drivers for this: first increases in clock speed and improvements in architecture (particularly Instruction Level Parallelism) and second massive increases in parallelism. In 1993 the TOP500 list still contained machines with only one processor, in November 2015 the smallest system has over 3700 cores, the largest has over 3 million cores. The first of these drivers has largely stalled as clock speeds have peaked at around 2-3 GHz due to power density limitations. Instruction level parallelism has also peaked at around 4-8 instructions per clock cycle; memories are not fast enough to provide enough operands to justify greater values. Further performance increase into the future is therefore expected to be driven solely by an increase in parallelism, through larger and larger number of processor cores.

Continuing the current exponential growth towards exaflop (10^{18} operations per second) performance, specifically requires a substantial reduction in power consumption (by ~ 100 -fold) to keep the power costs of HPC systems within reasonable limits. If these power efficiency constraints are lifted to achieve exascale systems there are two major impacts for ocean modelling. First is the prospect of a single ocean model running at exascale performance levels on e.g. 100 million cores. Alongside this there would be a knock-on effect as, for example, petascale systems become available with 100,000 cores in a single rack, consuming only ~ 100 kW.

To use the UK research community perspective as a practical example, Figure 9 shows the increase in the peak performance of the UK Research Council's (RCUK) HPC facility, from HPCx in 2006, through the four phases of Hector to the current machine Archer². The peak performance of this facility has increased exponentially over the past ~ 8 years. Given this trend has flattened off since the rapid increase between HPCx and Hector Phase 2a, the conservative estimate is to extrapolate the trend from Phase 2a to Archer Phase 2. This gives a peak performance of ~ 13 times Archer Phase 2 by 2019 (32Pflop/s) and ~ 745 times by 2023 (610Pflop/s). This closely follows the TOP500 trends, and predicts the UK maintains a performance about a factor of ten lower than the US at any one time (or lags by 3-4 years). There are of course many unknowns in this projection such as the size of the overall research community and share of the resource which the marine effort may receive. Nonetheless, this usefully quantifies the often quoted remarks around continually increasing computer power and puts bounds on what may be expected.

¹ <http://www.top500.org/>

² www.archer.ac.uk



In terms of ocean model design, to effectively utilise large numbers of cores, codes will have to extract very high degrees of parallelism from the underlying numerical algorithms. This requires at least three-way nested parallelism with high-level coarse-grained parallelism at the node level probably using MPI, multi-threading on a node using OpenMP or OpenAcc, and fine-grained parallelism within a core, e.g. vectorisation at the loop level. Memory management will become increasingly

5

important. The size of memory cannot increase to match the numbers of cores, on ground of cost and power, and the amount of memory per core is expected to reduce significantly (although memory per core is still relatively stable in the example presented here; Figure 9). Memory bandwidth per core and interconnect speed per core is also expected to drop. Algorithm design must therefore focus on management and movement of data in memory and between nodes.

10

Hence exploiting Petascale or Exascale levels of performance will require substantial algorithmic development to achieve the required level of concurrency. The layered approach to software design (Ford et al., In Press) provides one way to achieve this, while retaining code that can be developed by an ocean modeller.

To link the scale analysis and the computational issues, Table 3 lists a set of possible future model configurations, and an estimate of their relative cost with and without a timestep penalty. The relative cost is calculated by:

$$C = \frac{N}{N_{25}} \frac{L_{\min 25}}{L_{\min}} S, \quad (5)$$

15

where N is the total number of grid cells in a configuration defined by L_{\min} , and N_{25} and $L_{\min 25}$ are the reference values for nominal $1/4^\circ$ global NEMO configuration, ORCA025. S is a factor for models that need unstructured meshes. We take $S=5$ based on scaled run times of FVCOM and NEMO simulations for the northwest European continental shelf. This simplistic cost-model ignores all the real-world issues that would have to be faced, notably the changing balance between computation, memory access and communication, and also all arising data handling and storage issues.

20

Five quasi-uniform structured meshes, four unstructured mesh multiscale mesh options and an example of a block refined multiscale case are considered. To estimate when these could become routine models, an exponential fit to the growth of RCUK computer peak performance (Figure 9) is used so:

$$Y = \text{int}(\log_{10}(C)/P + Y_0), \quad (6)$$

25

taking the $1/4^\circ$ model in 2011 as a base line (Y_0) for a ‘routine’ high performance global physical oceanography research model. From Figure 9 $P=0.258 \text{ yr}^{-1}$ (i.e. doubling every ~ 1.2 years). So, for example in 2016 a $1/12^\circ$ model uses a comparable fraction of the total computer resource available as a $1/4^\circ$ model in 2011. There are many caveats to these estimates, not least the scientific development time needed to achieve the various stages, but they do serve as a reasonable guide to either encourage or constrain aspirations. It also highlights the importance of trying to alleviate the timestep constraints in multiscale models. A key milestone in this growth is a $1/12^\circ$ global model refined to $1/72^\circ$ to resolve coastal-ocean processes. This represents the amalgamation of the current state of the art of global and regional scale coastal-ocean modelling. With an unstructured mesh multiscale approach, this would be comparable to a $1/4^\circ$ model in 2011 by 2024, compared to block refined multiscale approach by 2022, and 2026 for a $1/72^\circ$ global model. This sets a clear challenge for ocean model developers and computer scientists to develop an efficient and accurate multiscale approach by this date. The trade-off here is between: numerical accuracy, lack of computational modes, ease of use and computational efficiency for the

30

structured grid, versus flexibility, improved coastline and longevity of a model for the unstructured grid case. The considerations above have focused on high resolution physical ocean models, e.g. as part of a coupled climate model or an operational forecast system. For Earth System Models with complex marine and land surface ecosystem and atmospheric chemistry components, we must accept that the ‘routine’ model of today (2016) is a 1° resolution ocean. The scaling then suggests that a $1/12^\circ$ global and a $1/12^\circ$ global model refined to $1/72^\circ$ would not have a comparable computational cost to a

40

1° ocean model until 2027 and 2035 respectively. This suggests options to improve the coastal-ocean in centennial scale



ESM simulations (e.g. for fully coupled carbon cycle simulations) will remain highly parameterised for at least the next decade, and for fine scale processes, two decades.

These results need to be seen alongside the needs of the open-ocean model. For example, Griffies et al (2009) note (in the context of mesoscale eddies): “There is no obvious place where grid resolution is unimportant”. Multiscale approaches can be applied to targeted regions of the open-ocean (Sein et al., 2016) to test this assertion, but an analysis of this issue is beyond the scope of the present study. Hence, unless very efficient methods of multiscale modelling are developed the added benefits of the higher resolution global model (e.g. improved Gulf Stream separation) are likely to outweigh the marginal improvements in efficiency achievable by a multiscale method if only modest coastal-ocean representation is required. If fine resolution coastal-ocean representation is desirable then the scaling favours multiscale modelling.

10

5. Conclusions

The analysis and investigation presented here suggest the prospects for improving the representation of the coastal-ocean in global models are now promising. We can identify three concurrent avenues of development to achieve this. Firstly, global models are now routinely run at the horizontal resolution of past shelf sea model simulations that capture many of the pertinent scales, and with dynamics that allow the representation of relevant processes, such as split-explicit time stepping rather than long wave-filtered or implicit approaches. In this case some (comparatively) straightforward developments can be included in the simulations to significantly improve the representation of the coastal-ocean. These are: i) including tides, their generating forces, self-attraction and loading and wave drag effects; ii) using vertical coordinate systems that retain resolution in shallow water, resolve the benthic boundary and allow smooth flow over steep topography; iii) adopting vertical mixing schemes that represent mixing at the surface, pycnocline and benthic boundary layers. These are all existing features of regional ocean models and the general challenge here is ensuring the introduction of these features does not compromise the deep and open ocean simulation, or significantly increase the computational costs. Further developments to achieve this are likely, for example through non-diffusive advection schemes and quasi-isopycnal vertical coordinates.

The second area of development is the continued refinement of horizontal resolution to the point that the pertinent scales are well resolved (estimated to be ~1.5km). This is the case in the current generation of region models, and the analysis presented here suggests it would be computationally practical in about a decade’s time. The options considered here, in very general terms are: a continued refinement of the quasi-uniform structured mesh, some form of unstructured mesh (presumed to be either finite element or volume), or else a multi-blocking refinement (whereby rectangular regions are refined to a fraction of the parent mesh and two-way coupled to it). The very simple cost-model we consider here puts these options at a ratio of about 10:3:1 respectively, with the cheapest (multi-block) being ~30 times more expensive than the 1/12° unrefined model.

The final area of development, and by no means the least important, is the improved representation of the coastal-oceans through improved process parameterisation. This essentially uses fundamental theoretical and empirical understanding to make up for deficiencies in the dynamical approach and the computational resource. This covers both processes that would not be resolved by any scales considered here and the cases where significant horizontal refinement is not practical (e.g. centennial scale ESM’s). Particular areas that deserve attention are: tidal mixing, topography and coastlines, horizontal mixing schemes that account for the large change in scales at the ocean margins, and river plumes. Given that the scale analysis presented here suggests we may be one or two decades away from a well-resolved coastal-ocean routinely run in fully coupled complex ESM’s, then these parameterisations are paramount.

This conclusion describes three complementary strands of work, which together have the potential to make substantial progress on our ability to model the coastal-ocean at a global scale, and so our ability to simulate global change and its impact on the societally pressing questions.



6. Code and data availability

NEMO model code used to run the Northern North Atlantic Model configuration to produce Figure 5 can be obtained from:

forge.ipsl.jussieu.fr/ipsl/forge/projets/nemo/svn/branches/NERC/dev_r3874_FASTNET

Data used to prepare Figures 1a-c, 2, 6, 7, 8 and Figure 5 are provided at

5 ftp://ftp.nerc-liv.ac.uk/pub/general/jth/GMD_Holt_GlobalCoasts/

In files respectively:

[GMD_Holt_GlobalCoasts_ORCA0083-N01_RR_data.nc](#) and [GMD_Holt_GlobalCoasts_PEA200_data.nc](#).

Data used for Figure 1a from: volkov.oce.orst.edu/tides/TPXO7.2.html, and for Figure 3 from:

www.cgd.ucar.edu/cas/catalog/surface/dai-runoff/coastal-stns-Vol-monthly_Constructed_wateryr-v2-updated-oct2007.nc

10 Figure 4 uses EN4.0.2 profile data from www.metoffice.gov.uk/hadobs/en4/download-en4-0-2.html.

Information for Figure 9 was obtained from www.hpcx.ac.uk/services/hardware/, www.hector.ac.uk/service/hardware/ and www.archer.ac.uk/.

7. Acknowledgements

This work was supported by the NERC Next Generation Ocean Dynamical Core Roadmap Project, and the National

15 Capability programme in ocean modelling at NOC and PML. Allen is supported by the NERC Integrated Modelling for Shelf Seas Biogeochemistry Programme. Hewitt and Woods were supported by the Joint UK DECC/Defra Met Office Hadley Centre Climate Programme (GA01101).

References

- Adcroft, A., Hill, C., and Marshall, J.: Representation of topography by shaved cells in a height coordinate ocean model,
20 Monthly Weather Review, 125, 2293-2315, 10.1175/1520-0493(1997)125<2293:rotbnc>2.0.co;2, 1997.
- Adcroft, A.: Representation of topography by porous barriers and objective interpolation of topographic data, Ocean Modelling, 67, 13-27, <http://dx.doi.org/10.1016/j.ocemod.2013.03.002>, 2013.
- Aksenov, Y., Ivanov, V. V., Nurser, A. J. G., Bacon, S., Polyakov, I. V., Coward, A. C., Naveira-Garabato, A. C., and Beszczynska-Moeller, A.: The Arctic Circumpolar Boundary Current, Journal of Geophysical Research: Oceans, 116,
25 C09017, 10.1029/2010jc006637, 2011.
- Allen, J. I., Aiken, J., Anderson, T. R., Buitenhuis, E., Cornell, S., Geider, R., Haines, K., Hirata, T., Holt, J., Le Quéré, C., Hardman-Mountford, N., Ross, O. N., Sinha, B., and While, J.: Marine ecosystem models for earth systems applications: The MarQUEST experience, Journal of Marine Systems, 81, 19-33, 2010.
- Arbic, B. K., Richman, J. G., Shriver, J. F., Timko, P. G., Metzger, E. J., and Wallcraft, A. J.: Global modeling of internal
30 tides within an eddy ocean general circulation model., Oceanography, 25, 20-29, 2012.
- Avicola, G., and Huq, P.: Scaling Analysis for the Interaction between a Buoyant Coastal Current and the Continental Shelf: Experiments and Observations, Journal of Physical Oceanography, 32, 3233-3248, 10.1175/1520-0485(2002)032<3233:safitib>2.0.co;2, 2002.
- Badin, G., Williams, R. G., Holt, J. T., and Fernand, L. J.: Are mesoscale eddies in shelf seas formed by baroclinic instability
35 of tidal fronts?, J. Geophys. Res.-Oceans, 114, C10021, C10021
10.1029/2009jc005340, 2009.
- Baines, P. G.: ON INTERNAL TIDE GENERATION MODELS, Deep-Sea Research Part a-Oceanographic Research Papers, 29, 307-338, 10.1016/0198-0149(82)90098-x, 1982.



- Barange, M., Merino, G., Blanchard, J. L., Scholtens, J., Harle, J., Allison, E. H., Allen, J. I., Holt, J., and Jennings, S.: Impacts of climate change on marine ecosystem production in societies dependent on fisheries, *Nature Clim. Change*, 4, 211-216, 10.1038/nclimate2119
<http://www.nature.com/nclimate/journal/v4/n3/abs/nclimate2119.html#supplementary-information>, 2014.
- 5 Barrón, C., and Duarte, C. M.: Dissolved organic carbon pools and export from the coastal ocean, *Global Biogeochemical Cycles*, 29, 1725-1738, 10.1002/2014gb005056, 2015.
- Bauer, J. E., Cai, W.-J., Raymond, P. A., Bianchi, T. S., Hopkinson, C. S., and Regnier, P. A. G.: The changing carbon cycle of the coastal ocean, *Nature*, 504, 61-70, 10.1038/nature12857, 2013.
- Bryan, F., Dennis, J., MacCready, P., and M., W.: Collaborative Project: Improving the Representation of Coastal and
- 10 Estuarine Processes in Earth System Models, 2015.
- Chen, C. S., Liu, H. D., and Beardsley, R. C.: An unstructured grid, finite-volume, three-dimensional, primitive equations ocean model: Application to coastal ocean and estuaries, *Journal of Atmospheric and Oceanic Technology*, 20, 159-186, 2003.
- Chen, C. T. A., and Borges, A. V.: Reconciling opposing views on carbon cycling in the coastal ocean: Continental shelves
- 15 as sinks and near-shore ecosystems as sources of atmospheric CO₂, *Deep-Sea Res. Part II-Top. Stud. Oceanogr.*, 56, 578-590, 10.1016/j.dsr2.2009.01.001, 2009.
- Colella, P., and Woodward, P. R.: The Piecewise Parabolic Method (PPM) for Gas-Dynamical Simulations, *Journal of Computational Physics*, 54, 174-201, 1984.
- Curchitser, E. N., Haidvogel, D. B., Hermann, A. J., Dobbins, E. L., Powell, T. M., and Kaplan, A.: Multi-scale modeling of
- 20 the North Pacific Ocean: Assessment and analysis of simulated basin-scale variability (1996-2003), *J. Geophys. Res.-Oceans*, 110, C11021
 10.1029/2005jc002902, 2005.
- Daewel, U., and Schrum, C.: Simulating long-term dynamics of the coupled North Sea and Baltic Sea ecosystem with ECOSMO II: Model description and validation, *Journal of Marine Systems*, 119, 30-49,
- 25 <http://dx.doi.org/10.1016/j.jmarsys.2013.03.008>, 2013.
- Dai, A., Qian, T., Trenberth, K. E., and Milliman, J. D.: Changes in continental freshwater discharge from 1948-2004. , *J. Climate*, 22, 2773-2791, 2009.
- Danilov, S.: Ocean modeling on unstructured meshes, *Ocean Modelling*, 69, 195-210, 10.1016/j.ocemod.2013.05.005, 2013.
- Danilov, S., and Androsov, A.: Cell-vertex discretization of shallow water equations on mixed unstructured meshes, *Ocean*
- 30 *Dynamics*, 65, 33-47, 10.1007/s10236-014-0790-x, 2015.
- Debreu, L., and Blayo, E.: Two-way embedding algorithms: a review, *Ocean Dynamics*, 58, 415-428, 10.1007/s10236-008-0150-9, 2008.
- Debreu, L., Marchesiello, P., Penven, P., and Cambon, G.: Two-way nesting in split-explicit ocean models: Algorithms, implementation and validation, *Ocean Modelling*, 49-50, 1-21, <http://dx.doi.org/10.1016/j.ocemod.2012.03.003>, 2012.
- 35 Ducheux, A., Frajka-Williams, E., Castro, N., Hirschi, J., and Coward, A.: Seasonal to interannual variability in density around the Canary Islands and their influence on the Atlantic meridional overturning circulation at 26°N, *Journal of Geophysical Research: Oceans*, 119, 1843-1860, 10.1002/2013jc009416, 2014.
- Egbert, G. D., and Erofeeva, S. Y.: Efficient inverse Modeling of barotropic ocean tides, *Journal of Atmospheric and Oceanic Technology*, 19, 183-204, 10.1175/1520-0426(2002)019<0183:eimob>2.0.co;2, 2002.
- 40 Ford, R., Glover, M. J., Ham, D. A., Maynard, C. M., Pickles, S. M., Riley, G. D., and Wood, N.: Gung Ho: A code design for weather and climate prediction on exascale machines, in *Exascale Applications and Software Conference, EASC2013*, Edinburgh, 9th-11th April 2013, to appear in a special edition of the journal *Advances in Engineering Software*, In Press.



- Gent, P. R., and McWilliams, J. C.: Isopycnal mixing in ocean circulation models., *Journal of Physical Oceanography*, 20, 150-155, 1990.
- Good, S. A., Martin, M. J., and Rayner, N. A.: EN4: Quality controlled ocean temperature and salinity profiles and monthly objective analyses with uncertainty estimates, *Journal of Geophysical Research: Oceans*, 118, 6704-6716, 10.1002/2013jc009067, 2013.
- Gordon, C., Cooper, C., Senior, C. A., Banks, H., Gregory, J. M., Johns, T. C., Mitchell, J. F. B., and Wood, R. A.: The simulation of SST, sea ice extents and ocean heat transports in a version of the Hadley Centre coupled model without flux adjustments, *Climate Dynamics*, 16, 147-168, 2000.
- Gräwe, U., Holtermann, P., Klingbeil, K., and Burchard, H.: Advantages of vertically adaptive coordinates in numerical models of stratified shelf seas, *Ocean Modelling*, 92, 56-68, <http://dx.doi.org/10.1016/j.ocemod.2015.05.008>, 2015.
- Greenberg, D. A., Dupont, F., Lyard, F. H., Lynch, D. R., and Werner, F. E.: Resolution issues in numerical models of oceanic and coastal circulation, *Continental Shelf Research*, 27, 1317-1343, 10.1016/j.csr.2007.01.023, 2007.
- Griffies, S. M., Adcroft, A., Banks, H., and al, e.: Problems and prospects in large-scale ocean circulation models, *Proceedings of OceanObs'09: Sustained Ocean Observations and Information for Society*, doi: 10.5270/OceanObs5209.cwp.5238 2009.
- Griffiths, R. W., and Linden, P. F.: Laboratory experiments on fronts Part I: Density Driven Boundary Currents, *Geophysical and Astrophysical Fluid Dynamics*, 19, 159-187, 1982.
- Griffiths, S. D.: Kelvin wave propagation along straight boundaries in C-grid finite-difference models, *Journal of Computational Physics*, 255, 639-659, 10.1016/j.jcp.2013.08.040, 2013.
- Gröger, M., Maier-Reimer, E., Mikolajewicz, U., Moll, A., and Sein, D.: NW European shelf under climate warming: implications for open ocean – shelf exchange, primary production, and carbon absorption, *Biogeosciences Discuss.*, 9, 16625-16662, doi:10.5194/bgd-16629-16625-2012, 2012.
- Hallberg, R.: Using a resolution function to regulate parameterizations of oceanic mesoscale eddy effects, *Ocean Modelling*, 72, 92-103, <http://dx.doi.org/10.1016/j.ocemod.2013.08.007>, 2013.
- Hecht, M. W., and Smith, R. D.: Toward a physical understanding of the North Atlantic: A review of model studies in an eddying regime, in: *Ocean Modeling in an Eddying Regime*, *Geophys. Monogr. Ser.*, edited by: M. W. Hecht, M. W., and Hasumi, H., AGU, 2008.
- Heuzé, C., Heywood, K. J., Stevens, D. P., and Ridley J.K.: Southern Ocean bottom water characteristics in CMIP5 models, *Geophysical Research Letters*, 40(7), 1409 - 1414., 2013.
- Hewitt, H. T., Copsey, D., Culverwell, I. D., Harris, C. M., Hill, R. S. R., Keen, A. B., McLaren, A. J., and Hunke, E. C.: Design and implementation of the infrastructure of HadGEM3: the next-generation Met Office climate modelling system, *Geoscientific Model Development*, 4, 223-253, 10.5194/gmd-4-223-2011, 2011.
- Hill, A. E., Brown, J., Fernand, L., Holt, J., Horsburgh, K. J., Proctor, R., Raine, R., and Turrell, W. R.: Thermohaline circulation of shallow tidal seas, *Geophysical Research Letters*, 35, 2008.
- Hobday, A. J., and Pecl, G. T.: Identification of global marine hotspots: sentinels for change and vanguards for adaptation action, *Rev. Fish. Biol. Fish.*, 24, 415-425, 10.1007/s11160-013-9326-6, 2014.
- Holt, J., and Umlauf, L.: Modelling the tidal mixing fronts and seasonal stratification of the Northwest European Continental shelf, *Continental Shelf Research*, 28, 887-903, 2008.
- Holt, J., Harle, J., Proctor, R., Michel, S., Ashworth, M., Batstone, C., Allen, J. I., Holmes, R., Smyth, T., Haines, K., Bretherton, D., and Smith, G.: Modelling the global coastal-ocean Phi. *Trans Roy. Soc. Lon. A*, doi:10.1098/rsta.2008.0210, 2009a.



- Holt, J., Wakelin, S., and Huthnance, J.: Down-welling circulation of the northwest European continental shelf: A driving mechanism for the continental shelf carbon pump, *Geophysical Research Letters*, 36, L14602
doi:10.1029/2009GL038997, L14602
10.1029/2009gl038997, 2009b.
- 5 Holt, J., Wakelin, S., Lowe, J., and Tinker, J.: The potential impacts of climate change on the hydrography of the northwest European Continental shelf., *Progress in Oceanography*, 86, 361-379, doi:10.1016/j.pocean.2010.05.003 2010.
Holt, J., New, A., Liu, H., Coward, A., Pickles, S., and Ashworth, M.: Next Generation Ocean Dynamical Core Roadmap Project: Final Report <http://www.nerc.ac.uk/research/funded/programmes/ngwcp/ocean-roadmap-report/>, 2013.
- 10 Holt, J., Allen, J. I., Anderson, T. R., Brewin, R., Butenschon, M., Harle, J., Huse, G., Lehodey, P., Lindemann, C., Memery, L., Salihoglu, B., Senina, I., and Yool, A.: Challenges in integrative approaches to modelling the marine ecosystems of the North Atlantic: Physics to Fish and Coasts to Ocean, *Progress in Oceanography*, doi:10.1016/j.pocean.2014.04.024, 2014.
Holt, J., Huthnance, J., Sharples, J., James, I., Maqueda, M. A. M., Willmott, A. J., and Mooers, C. N. K.: Coastal Ocean Circulation Dynamics, in: *Coupled Coastal Wind-Wave-Current Dynamics*, edited by: Craig, P., Mooers, C., and Norden, H., Cambridge University Press, In Press.
- 15 Holt, J. T., and Proctor, R.: The seasonal circulation and volume transport on the northwest European continental shelf: a fine-resolution model study, *Journal of Geophysical Research*, 113, C06021, doi:06010.01029/02006JC004034, 2008.
Huthnance, J. M.: Circulation, exchange and water masses at the ocean margin: the role of physical processes at the shelf edge, *Progress in Oceanography*, 35, 353-431, 1995.
Ilicak, M., Adcroft, A. J., Griffies, S. M., and Hallberg, R. W.: Spurious diapycnal mixing and the role of momentum closure., *Ocean Modelling* 45-46, 37-58 , doi:10.106/j.ocemod.2011.2010.2003., 2012.
- 20 Ingram, D. M., Causon, D. M., and Mingham, C. G.: Developments in Cartesian cut cell methods, *Mathematics and Computers in Simulation*, 61, 561-572, [http://dx.doi.org/10.1016/S0378-4754\(02\)00107-6](http://dx.doi.org/10.1016/S0378-4754(02)00107-6), 2003.
Leclair, M., and Madec, G.: (z)over-tilde-Coordinate, an Arbitrary Lagrangian-Eulerian coordinate separating high and low frequency motions, *Ocean Modelling*, 37, 139-152, 10.1016/j.ocemod.2011.02.001, 2011.
- 25 Legrand, S., Deleersnijder, E., Delhez, E., and Legat, V.: Unstructured, anisotropic mesh generation for the Northwestern European continental shelf, the continental slope and the neighbouring ocean, *Continental Shelf Research*, 27, 1344-1356, 10.1016/j.csr.2007.01.009, 2007.
Lin, J.-L.: The Double-ITCZ Problem in IPCC AR4 Coupled GCMs: Ocean–Atmosphere Feedback Analysis, *Journal of Climate*, 20, 4497-4525, 10.1175/jcli4272.1, 2007.
- 30 Luneva, M. V., Harle, J. D., Aksenov, Y., and Holt, J. T.: The effects of tides on the water mass mixing and sea ice in the Arctic Ocean., *Journal of Geophysical Research*, doi:10.1002/2014JC010310, 2015.
Maraldi, C., Chanut, J., Levier, B., Refray, G., Ayoub, N., De Mey, P., Lyard, F., Cailleau, S., Drévilion, M., A. Fanjul, E. A., Sotillo, M. G., Marsaleix, P., and Team, t. M.: NEMO on the shelf: assessment of the Iberia–Biscay–Ireland configuration, *Ocean Sci. Discuss.*, 9, 499-583, 2012.
- 35 Marsaleix, P., Auclair, F., and Estournel, C.: Considerations on open boundary conditions for regional and coastal ocean models, *Journal of Atmospheric and Oceanic Technology*, 23, 1604-1613, 10.1175/jtech1930.1, 2006.
Marzocchi, A., Hirschi, J. J. M., Holliday, N. P., Cunningham, S. A., Blaker, A. T., and Coward, A. C.: The North Atlantic subpolar circulation in an eddy-resolving global ocean model, *Journal of Marine Systems*, 142, 126-143, 10.1016/j.jmarsys.2014.10.007, 2015.
- 40 Mason, E., Molemaker, J., Shchepetkin, A. F., Colas, F., McWilliams, J. C., and Sangra, P.: Procedures for offline grid nesting in regional ocean models, *Ocean Modelling*, 35, 1-15, 10.1016/j.ocemod.2010.05.007, 2010.



- Merino, G., Barange, M., Blanchard, J. L., Harle, J., Holmes, R., Allen, I., Allison, E. H., Badjeck, M. C., Dulvy, N. K., Holt, J., Jennings, S., Mullon, C., and Rodwell, L. D.: Can marine fisheries and aquaculture meet fish demand from a growing human population in a changing climate?, *Global Environmental Change*, 22, 795-806, 2012.
- Müller, M., Haak, H., Jungclaus, J. H., Sündermann, J., and Thomas, M.: The effect of ocean tides on a climate model simulation. , *Ocean Modelling*, 35, 304-313, 2010.
- 5 Munk, W. H., and Wunsch, C.: Abyssal recipes II: energetics of tidal and wind mixing, *Deep Sea Res., Part II*, 45, 1977-2010, 1998.
- Nicholls, R. J.: Coastal flooding and wetland loss in the 21st Century: Changes under the SRES climate and socio-economic scenarios., *Global Environmental Change*, 14(1), 69-86, 2004.
- 10 Niwa, Y., and Hibiya, T.: Estimation of baroclinic tide energy available for deep ocean mixing based on three-dimensional global numerical simulations, *J. Oceanogr.*, 67, 493-502, 10.1007/s10872-011-0052-1, 2011.
- Nurser, A. J. G., and Bacon, S.: The Rossby radius in the Arctic Ocean, *Ocean Sci.*, 10, 967-975, 10.5194/os-10-967-2014, 2014.
- O'Dea, E. J., Arnold, A., Edwards, K. P., Furner, R., Hyder, P., Martin, M. J., Siddorn, J. R., Storkey, D., While, J., Holt, J.
- 15 T., and Liu, H.: An operational ocean forecast system incorporating NEMO and SST data assimilation for the tidally driven European North-West shelf, *Journal of Operational Oceanography*, 5(1), 3-17, 2012.
- Orsi, A. H., Johnson, G. C., and Bullister, J. L.: Circulation, mixing and production of Antarctic Bottom Water., *Progress in Oceanography*, 43(1), 55-109, 1999.
- Orsi, A. H.: Oceanography: recycling bottom waters., *Nat. Geosci.*, 3 (5), 307-309, 2010.
- 20 Palmer, M. R., Inall, M. E., and Sharples, J.: The physical oceanography of Jones Bank: A mixing hotspot in the Celtic Sea, *Progress in Oceanography*, 117, 9-24, 10.1016/j.pocean.2013.06.009, 2013.
- Peliz, A., Rosa, T. L., Santos, M. P., and Pissarra, J. L.: Fronts, jets, and counter-flows in the western Iberian upwelling system, *Journal of Marine Systems*, 35, 61-77, 2002.
- Polton, J. A.: Tidally induced mean flow over bathymetric features: a contemporary challenge for high-resolution wide-area
- 25 models, *Geophysical & Astrophysical Fluid Dynamics*, 1-9, 10.1080/03091929.2014.952726, 2014.
- Popova, E., Yool, A., Byfield, V., Cochrane, K., Coward, A. C., Salim, S. S., Gasalla, M. A., Henson, S. A., Hobday, A. J., Pecl, G., Sauer, W., and Roberts, M.: From global to regional and back again: common climate stressors of marine ecosystems relevant for adaptation across five ocean warming hotspots, *Global Change Biology*, n/a-n/a, 10.1111/gcb.13247, 2016.
- 30 Prather, M. J.: Numerical advection by conservation of 2nd-order moments, *J. Geophys. Res.-Atmos.*, 91, 6671-6681, 10.1029/JD091iD06p06671, 1986.
- Renner, A. H. H., Heywood, K. J., and Thorpe, S. E.: Validation of three global ocean models in the Weddell Sea, *Ocean Modelling*, 30, 1-15, 10.1016/j.ocemod.2009.05.007, 2009.
- Ringler, T., Petersen, M., Higdon, R. L., Jacobsen, D., Jones, P. W., and Maltrud, M.: A multi-resolution approach to global
- 35 ocean modeling, *Ocean Modelling*, 69, 211-232, <http://dx.doi.org/10.1016/j.ocemod.2013.04.010>, 2013.
- Rippeth, T. P., and Inall, M. E.: Observations of the internal tide and associated mixing across the Malin Shelf, *Journal of Geophysical Research*, 107, 3-1-3-3-1-15, 2002.
- Roberts, M. J., Marsh, R., New, A. L., and Wood, R. A.: An intercomparison of a Bryan-Cox type ocean model and an isopycnic ocean model. Part I: the subpolar gyre and high-latitude processes, *Journal of Physical Oceanography*, 26, 1495-
- 40 1527, 1996.
- Rykaczewski, R. R., and Dunne, J. P.: Enhanced nutrient supply to the California Current Ecosystem with global warming and increased stratification in an earth system model, *Geophysical Research Letters*, 37, L21606, DOI: 21610.21029/22010GL045019 L21606



- 10.1029/2010gl045019, 2010.
- Sein, D. V., Danilov, S., Biastoch, A., Durgadoo, J. V., Sidorenko, D., Harig, S., and Wang, Q.: Designing variable ocean model resolution based on the observed ocean variability, *Journal of Advances in Modeling Earth Systems*, n/a-n/a, 10.1002/2016ms000650, 2016.
- 5 Seitzinger, S. P., and Kroeze, C.: Global distribution of nitrous oxide production and N inputs in freshwater and coastal marine ecosystems, *Global Biogeochemical Cycles*, 12, 93-113, 10.1029/97gb03657, 1998.
- Seitzinger, S. P., Harrison, J. A., Dumont, E., Beusen, A. H. W., and Bouwman, A. F.: Sources and delivery of carbon, nitrogen, and phosphorus to the coastal zone: An overview of Global Nutrient Export from Watersheds (NEWS) models and their application, *Global Biogeochemical Cycles*, 19, Gb4s01
- 10 10.1029/2005gb002606, 2005.
- Shakhova, N., Semiletov, I., Salyuk, A., Yusupov, V., Kosmach, D., and Gustafsson, O.: Extensive Methane Venting to the Atmosphere from Sediments of the East Siberian Arctic Shelf, *Science*, 327, 1246-1250, 10.1126/science.1182221, 2010.
- Shapiro, G., Luneva, M., Pickering, J., and Storkey, D.: The effect of various vertical discretization schemes and horizontal diffusion parameterization on the performance of a 3-D ocean model: the Black Sea case study, *Ocean Sci.*, 9, 377-390,
- 15 10.5194/os-9-377-2013, 2013.
- Shchepetkin, A. F., and McWilliams, J. C.: A method for computing horizontal pressure-gradient force in an oceanic model with a nonaligned vertical coordinate, *J. Geophys. Res.-Oceans*, 108, 2003.
- Siddorn, J. R., and Furner, R.: An analytical stretching function that combines the best attributes of geopotential and terrain-following vertical coordinates, *Ocean Modelling*, 66, 1-13, 10.1016/j.ocemod.2013.02.001, 2013.
- 20 Simmons, H. L., Jayne, S. R., St Laurent, L. C., and Weaver, A. J.: Tidally driven mixing in a numerical model of the ocean general circulation, *Ocean Modelling*, 6, 245-263, 10.1016/s1463-5003(03)00011-8, 2004.
- Simpson, J. H., and Hunter, J. R.: Fronts in the Irish Sea, *Nature*, 250, 404-406, 1974.
- Simpson, J. H., and Bowers, D.: Models of stratification and frontal movement in shelf seas, *Deep Sea Research*, 28, 727-738, 1981.
- 25 Smagorinsky, J.: General circulation experiments with the primitive equations, *Monthly Weather Review*, 91, 99-164, 1963.
- St. Laurent, L. C., Simmons, H. L., and Jayne, S. R.: Estimating tidally driven mixing in the deep ocean, *Geophysical Research Letters*, 29, 21-21-21-24, 10.1029/2002gl015633, 2002.
- Stammer, D., Ray, R. D., Andersen, O. B., Arbic, B. K., Bosch, W., Carrere, L., Cheng, Y., Chinn, D. S., Dushaw, B. D., Egbert, G. D., Erofeeva, S. Y., Fok, H. S., Green, J. A. M., Griffiths, S., King, M. A., Lapin, V., Lemoine, F. G., Luthcke, S.
- 30 B., Lyard, F., Morison, J., Muller, M., Padman, L., Richman, J. G., Shriver, J. F., Shum, C. K., Taguchi, E., and Yi, Y.: Accuracy assessment of global barotropic ocean tide models, *Reviews of Geophysics*, 52, 243-282, 10.1002/2014rg000450, 2014.
- Stepanov, V. N., and Hughes, C. W.: Parameterization of ocean self-attraction and loading in numerical models of the ocean circulation, *Journal of Geophysical Research: Oceans*, 109, C03037, 10.1029/2003jc002034, 2004.
- 35 Timmermann, R., Danilov, S., Schroter, J., Boning, C., Sidorenko, D., and Rollenhagen, K.: Ocean circulation and sea ice distribution in a finite element global sea ice-ocean model, *Ocean Modelling*, 27, 114-129, 10.1016/j.ocemod.2008.10.009, 2009.
- Tseng, Y. H., and Ferziger, J. H.: A ghost-cell immersed boundary method for flow in complex geometry, *Journal of Computational Physics*, 192, 593-623, 10.1016/j.jcp.2003.07.024, 2003.
- 40 Umlauf, L., and Burchard, H.: A generic length-scale equation for geophysical turbulence models, *Journal of Marine Research*, 61, 235-265, 10.1357/002224003322005087, 2003.



Wakelin, S. L., Holt, J. T., and Proctor, R.: The influence of initial conditions and open boundary conditions on shelf circulation in a 3D ocean-shelf model of the North East Atlantic, *Ocean Dynamics*, 59, 67-81 DOI: 10.1007/s10236-10008-10164-10233, 2009.

Willebrand, J., Barnier, B., Boning, C., Dieterich, C., Killworth, P. D., Le Provost, C., Jia, Y. L., Molines, J. M., and New, A. L.: Circulation characteristics in three eddy-permitting models of the North Atlantic, *Progress in Oceanography*, 48, 123-161, 10.1016/s0079-6611(01)00003-9, 2001.

Williams, K. D., Harris, C. M., Bodas-Salcedo, A., Camp, J., Comer, R. E., Copsy, D., Fereday, D., Graham, T., Hill, R., Hinton, T., Hyder, P., Ineson, S., Masato, G., Milton, S. F., Roberts, M. J., Rowell, D. P., Sanchez, C., Shelly, A., Sinha, B., Walters, D. N., West, A., Woollings, T., and Xavier, P. K.: The Met Office Global Coupled model 2.0 (GC2) configuration, *Geoscientific Model Development*, 8, 1509-1524, 10.5194/gmd-88-1509-2015, 2015.

Wobus, F., Shapiro, G. I., Huthnance, J. M., and Maqueda, M. A. M.: The piercing of the Atlantic Layer by an Arctic shelf water cascade in an idealized study inspired by the Storfjorden overflow in Svalbard, *Ocean Modelling*, 71, 54-65, 2013.

Wu, L. X., Cai, W. J., Zhang, L. P., Nakamura, H., Timmermann, A., Joyce, T., McPhaden, M. J., Alexander, M., Qiu, B., Visbeck, M., Chang, P., and Giese, B.: Enhanced warming over the global subtropical western boundary currents, *Nat. Clim. Chang.*, 2, 161-166, 10.1038/nclimate1353, 2012.

Yankovsky, A. E., and Chapman, D. C.: A simple theory for the fate of buoyant coastal discharges, *Journal of Physical Oceanography*, 27, 1386-1401, 1997.

Zhang, W. F. G., and Gawarkiewicz, G. G.: Dynamics of the direct intrusion of Gulf Stream ring water onto the Mid-Atlantic Bight shelf, *Geophysical Research Letters*, 42, 7687-7695, 10.1002/2015gl065530, 2015.

Zhang, W. G. F., Wilkin, J. L., and Chant, R. J.: Modeling the Pathways and Mean Dynamics of River Plume Dispersal in the New York Bight, *Journal of Physical Oceanography*, 39, 1167-1183, 10.1175/2008jpo4082.1, 2009.

Zhao, Z., Alford, M. H., and J.B., G.: Mapping Low-Mode Internal Tides from Multisatellite Altimetry. , *Oceanography*, 25(2), 42-51, 2012.

25 Table 1: Physical process horizontal scales in coastal and shelf seas

Process		Horizontal scale	Reference
Barotropic Tide	L_{bt}	$\sqrt{gH} / \max(f, \omega)$	(Huthnance, 1995)
Tidal excursion	L_e	U_T/ω	(Polton, 2014)
Topographic steered barotropic current	L_T	$H.(\nabla H)^{-1}$	(Greenberg et al., 2007)
Front/frontal jet, coastal upwelling	L_1	C_{iw}/f	(Huthnance, 1995)
Baroclinic eddy	L_E	πL_1	(Griffiths and Linden, 1982)
Internal wave/tide	L_{iw}	C_{iw}/ω	(Huthnance, 1995)
Coastal current/river plume	L_r	$(2Qf/g')^{1/2} (\nabla H)^{-1}$ $(2Qg')^{0.25}/f^{0.75}$	(Yankovsky and Chapman, 1997) (Avicola and Huq, 2002)

Here: U_T tidal current, ω frequency, H water depth, g gravitational acceleration, f Coriolis parameter, C_{iw} internal wave phase speed, Q riverine volume flux.

Table 2 A selection of current model grids

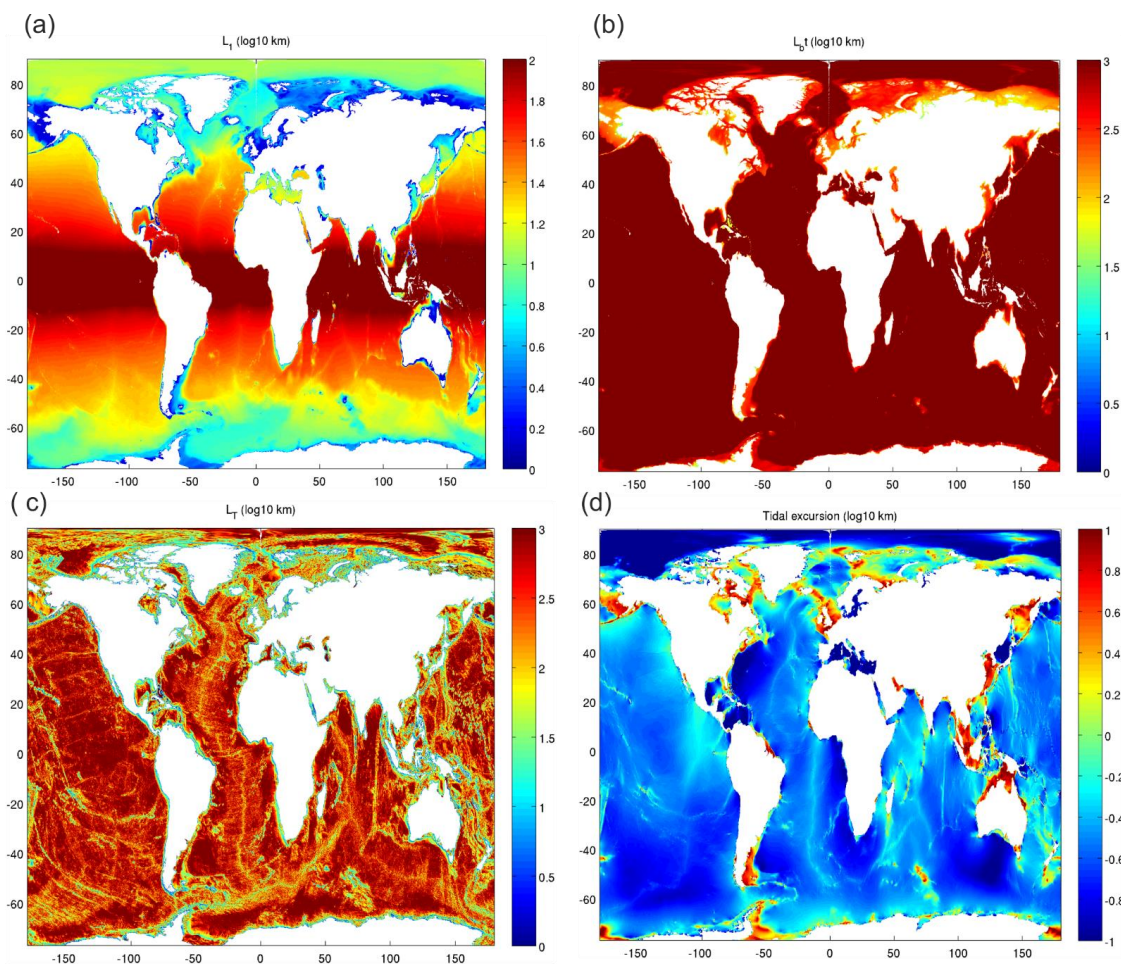


Nominal resolution	Scale at equator (km)	Global application	Coastal-ocean application	Examples
1°	111	Typical of Earth Systems Models CMIP4 and 5	NA	HadGEM3; (Hewitt et al., 2011), HadCM3; (Gordon et al., 2000)
1/4°	25	CMIP6 ESMs	Historical	HadGEM3(Williams et al., 2015)
1/12°	9.3	Next generation coupled	Shelf scale/ocean margin	ORCA12; (Marzocchi et al., 2015) AMM7; (O’Dea et al., 2012) AMM12; (Wakelin et al., 2009)
1/36°	3.5	Next generation forced	Shelf Scale	IBI (Maraldi et al., 2012) ECOSMO (Daewel and Schrum, 2013)
1/72°	1.5	NA	High res. shelf/coastal	HRCS (Holt and Proctor, 2008)

Table 3: Possible model grids, their costs (Eqn 5) and when they might be computationally equivalent to ORCA025 model (nominal 1/4°) in 2011 based on Eqn 6, from Figure 9. Unstructured grids are refined to the minimum of L_1 , L_{bt} , L_T according to Eqns. 3 and 4, and we assume are 5 times more expensive.

Global Grid	S/US	Vertical	Size (k cells)	Cost (time step) cf ORCA025	Cost (no time step)	When routine physics model
¼	S	75	905	1	1	2011
1/12	S	75	8,149	27	9	2016
1/36	S	100	73,342	972	108	2022
1/48	S	100	130,390	2304	192	2024
1/72	S	100	293,370	7776	432	2026
1/4+1/12	US	100	2,037	45	15	2017
1/12+1/36	US	100	10,910	723	80	2022
1/12+1/72	US	100	17,409	2307	128	2024
1/24+1/72	US	100	22,331	2960	164	2024
1/12+1/72	BL	100	45,558	791	67	2022

5 S= structured, US = unstructured, BL= blocked refined, e.g. using AGRIF



5 Figure 1 Global scales: a) 1st Baroclinic Rossby Radius; the maximum value calculated from monthly ORCA12 density profiles (each month being an average from 1981 to 2010) following Nurser and Bacon (2014), using the model run described by Marzochi et al (2015) ; b) Barotropic Rossby Radius calculated from ORCA12 bathymetry; c) Topographic scale calculated from ORCA12 bathymetry and mesh; d) Tidal excursion, calculated from TPXO barotropic tidal currents (Egbert and Erofeeva, 2002).

10

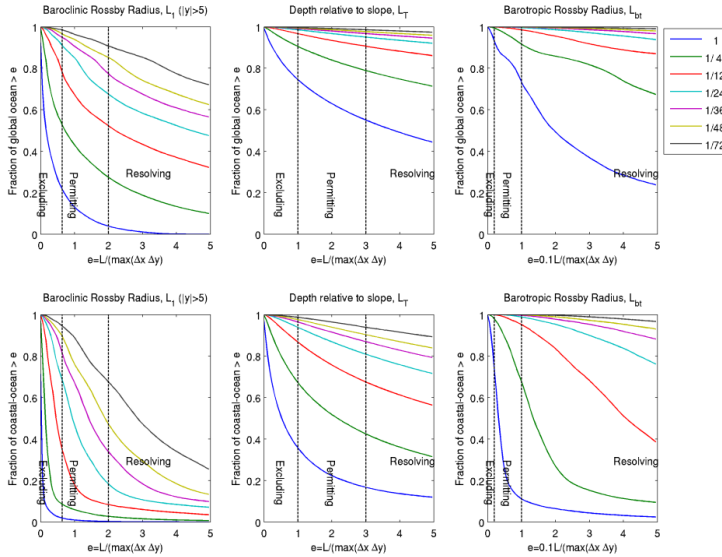


Figure 2 Cumulative distribution of the fraction of global (top) and coastal (bottom) ocean resolving L_1 , L_T , L_{bt} for different global model resolutions.

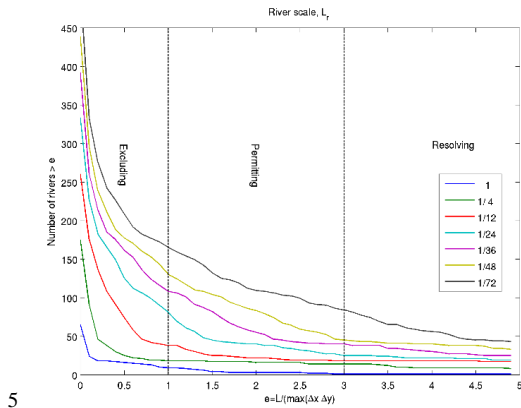
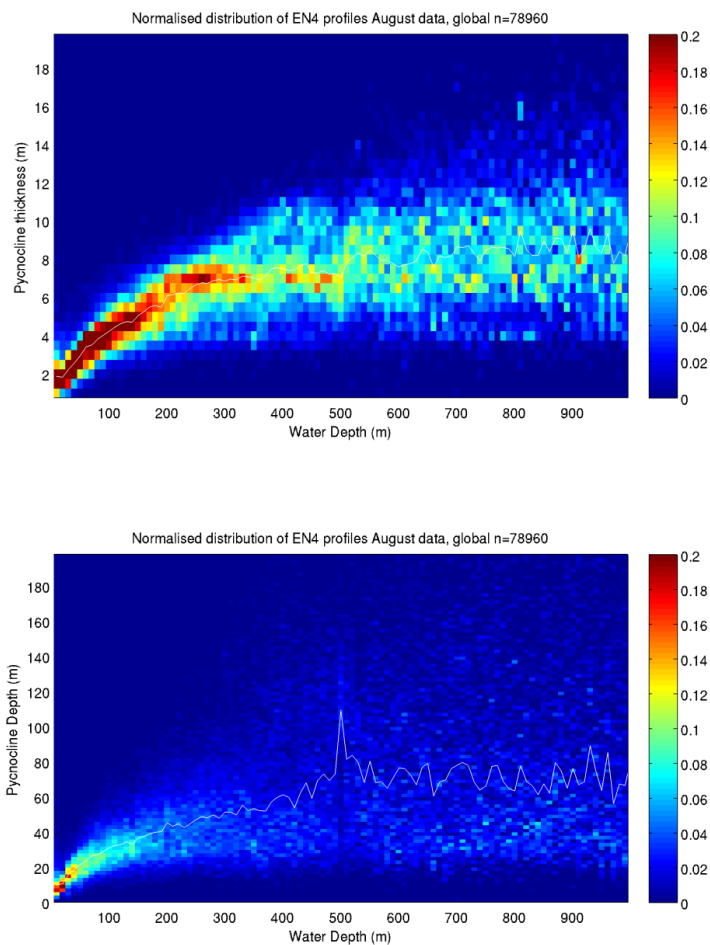


Figure 3 Cumulative distribution of number of rivers where the scale L_r is resolved at a particular level (e). Based on flow data from the 925 largest ocean-flowing rivers globally (Dai et al., 2009).



5 **Figure 4** Distributions of pycnocline thickness and depth (Eqn 2) from the global profile data set EN4. Profiles are counted at each bin of water depth and Z_T or Z_D , and normalised by the number of profiles at that water depth. Data are from August in each year from 1977 to 2015. Profiles with fewer than 10 data points in the vertical are discarded. The white line shows the median value at each depth bin.

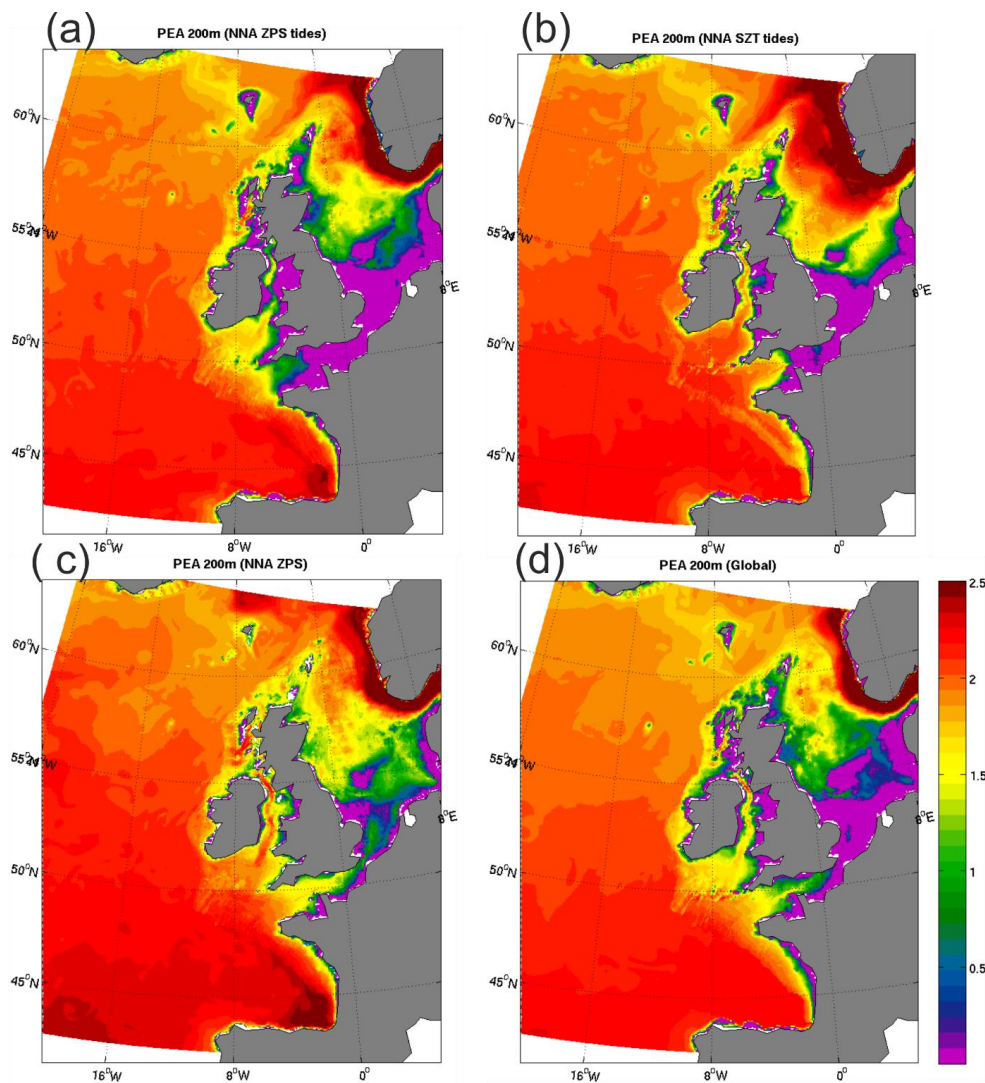


Figure 5 Potential energy anomaly focusing on NE Atlantic mean for June, July, and August in 1987. Results for three runs of the Northern North Atlantic NEMO configuration are shown, with the GLS vertical mixing scheme: A) Z Partial Steps with tides; B) Hybrid S-Z coordinate with tides; C) ZPS without tides. D) Results from the global ORCA12 model with the TKE mixing scheme and no tides. Plots show \log_{10} of PEA in Jm^{-3} , calculate to a maximum depth of the shallower of the sea bed or 200m.

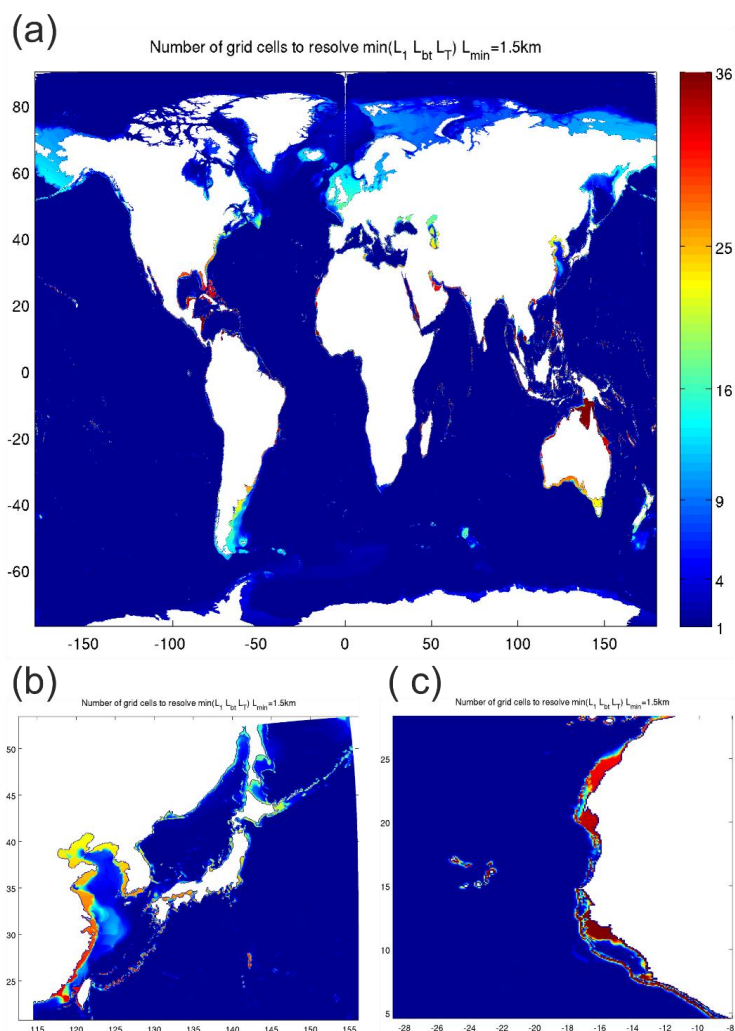


Figure 6 An example of how a $1/12^\circ$ global grid (a) might conceptually be refined to resolve the dominant scales. Parameter shown is number of cells needed in each global grid cell to resolve these scales down to a minimum scale of 1.5km, so ranges from 1 (no refinement) to $(72/12)^2=36$. Below are two example in more detail for (b) East Asia and (c) NW Africa.

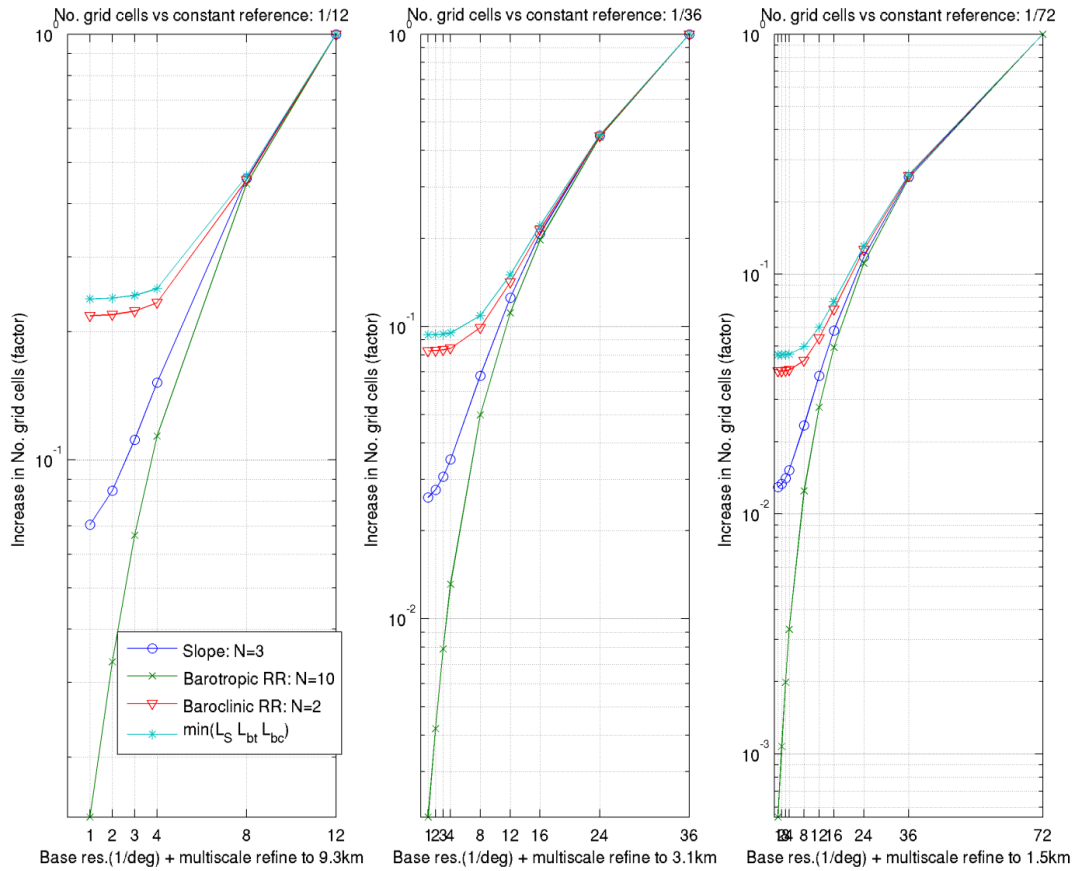


Figure 7 Number of grid cells to achieve process representation in shelf seas with a multiscale approach, relative to a refining global reference resolution of 1/12°, 1/36° and 1/72° and down to a minimum scale set by this global reference.

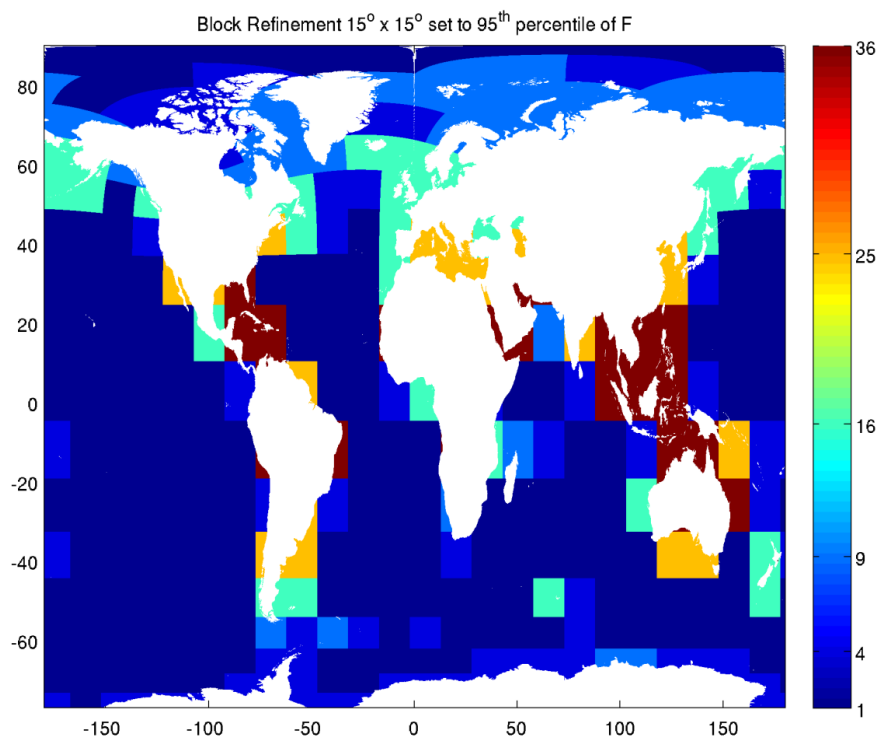


Figure 8 Refinement of $15^\circ \times 15^\circ$ blocks to the 95th percentile of the distribution of F^2 in each block. Set to $(\text{int}(F))^2$ to approximate refinement by an approach such as AGRIF.

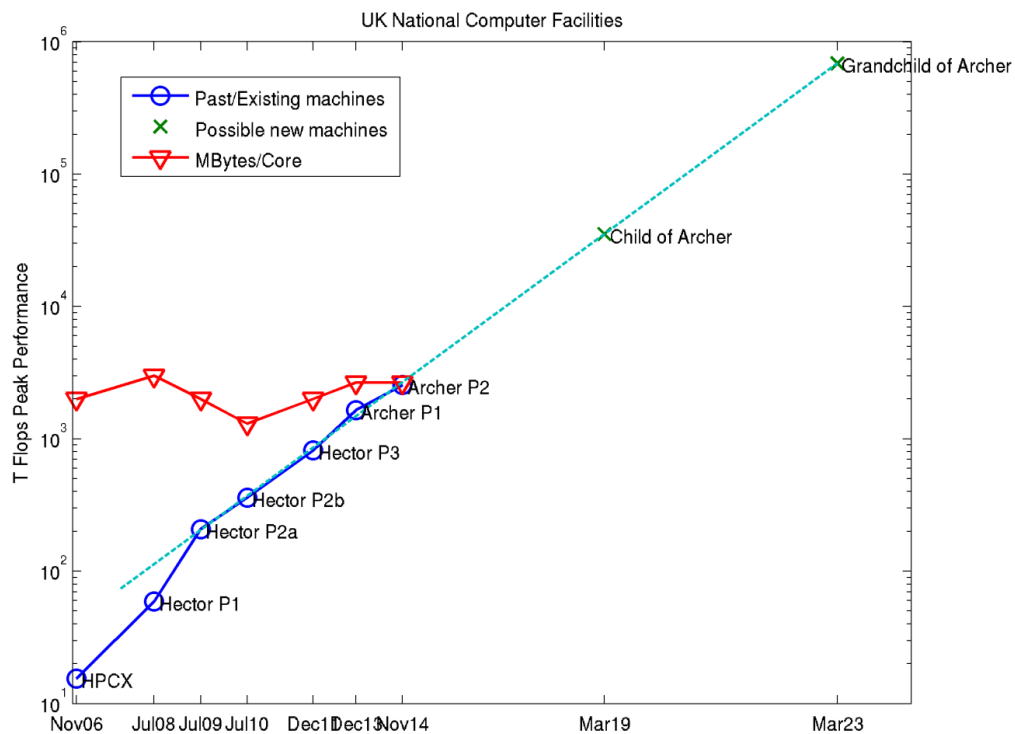


Figure 9 The UK research computer facility peak performance and memory per core. Also shown are two-projected possible future machines.

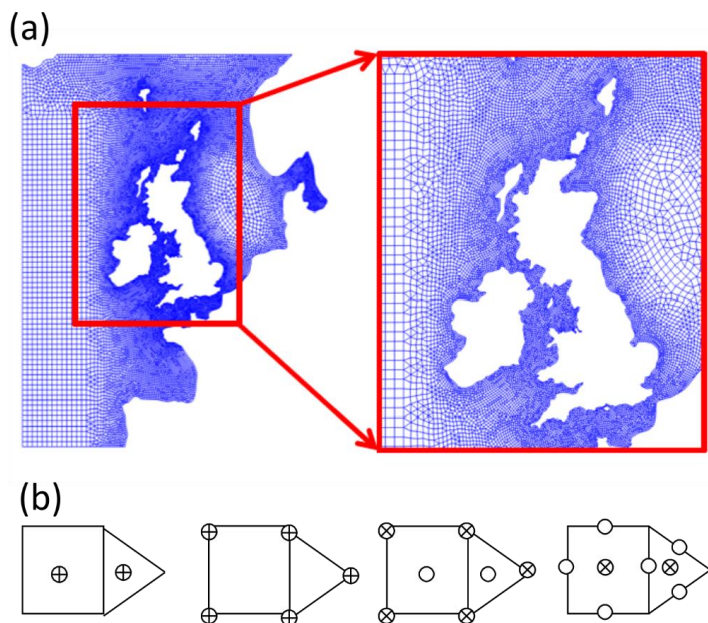


Figure 10 An example of mixed element unstructured mesh (a); Variable arrangement in a mixed triangle quadrilateral grid (b).
 From left to the right, we name them A, A1, B, C grid. \oplus Represents all variables, \otimes represents pressure/sea surface elevation, \circ
 5 represents full velocity in B-Grid and velocity components normal to the edge of polygons in C-Grid.